University of Groningen

β(2→6)-Type fructans attenuate proinflammatory responses in a structure dependent fashion via Toll-like receptors

Fernández-Lainez, C; Akkerman, R; Oerlemans, M.M.P.; Logtenberg, M.J.; Schols, H.A.; Silva Lagos, L.A.; López-Velázquez, G.; de Vos, Paul

Published in:
Carbohydrate Polymers

DOI:
10.1016/j.carbpol.2021.118893

IMPORTANT NOTE: You are advised to consult the publisher's version (publisher's PDF) if you wish to cite from it. Please check the document version below.

Document Version
Publisher's PDF, also known as Version of record

Publication date:
2022

Link to publication in University of Groningen/UMCG research database

Citation for published version (APA):
Fernández-Lainez, C., Akkerman, R., Oerlemans, M. M. P., Logtenberg, M. J., Schols, H. A., Silva Lagos, L. A., López-Velázquez, G., & de Vos, P. (2022). β(2→6)-Type fructans attenuate proinflammatory responses in a structure dependent fashion via Toll-like receptors. *Carbohydrate Polymers*, *277*, [118893]. https://doi.org/10.1016/j.carbpol.2021.118893

Copyright
Other than for strictly personal use, it is not permitted to download or to forward/distribute the text or part of it without the consent of the author(s) and/or copyright holder(s), unless the work is under an open content license (like Creative Commons).

The publication may also be distributed here under the terms of Article 25fa of the Dutch Copyright Act, indicated by the "Taverne" license. More information can be found on the University of Groningen website: https://www.rug.nl/library/open-access/self-archiving-pure/taverne-amendment.

Take-down policy
If you believe that this document breaches copyright please contact us providing details, and we will remove access to the work immediately and investigate your claim.

Downloaded from the University of Groningen/UMCG research database (Pure): http://www.rug.nl/research/portal. For technical reasons the number of authors shown on this cover page is limited to 10 maximum.

Carbohydrate Polymers xxx (xxxx) xxx

Contents lists available at ScienceDirect

Carbohydrate Polymers

journal homepage: www.elsevier.com/locate/carbpol

β(2→6)-Type fructans attenuate proinflammatory responses in a structure dependent fashion via Toll-like receptors

C. Fernández-Lainez [a,b,c,*], R. Akkerman [a], M.M.P. Oerlemans [a], M.J. Logtenberg [d], H.A. Schols [d], L.A. Silva-Lagos [a], G. López-Velázquez [e], P. de Vos [a]

[a] Immunoendocrinology, Division of Medical Biology, Department of Pathology and Medical Biology, University of Groningen and University Medical Center Groningen, Hanzeplein 1, 9700 RB Groningen, the Netherlands
[b] Laboratorio de Errores Innatos del Metabolismo y Tamiz, Instituto Nacional de Pediatría, Ciudad de México, Mexico
[c] Posgrado en Ciencias Biológicas, Universidad Nacional Autónoma de México UNAM, Ciudad de México, Mexico
[d] Laboratory of Food Chemistry, Wageningen University, Wageningen, the Netherlands
[e] Laboratorio de Biomoléculas y Salud Infantil, Instituto Nacional de Pediatría, Ciudad de México, Mexico

ARTICLE INFO

Keywords:
Branched-chain fructans
Functional food
Immunomodulation
Non-digestible carbohydrates
Toll-like receptors

ABSTRACT

Graminan-type fructans (GTFs) have demonstrated immune benefits. However, mechanisms underlying these benefits are unknown. We studied GTFs interaction with Toll-like receptors (TLRs), performed molecular docking and determined their impact on dendritic cells (DCs). Effects of GTFs were compared with those of inulin-type fructans (ITFs). Whereas ITFs only contained β(2→1)-linked fructans, GTFs showed higher complexity as it contains additional β(2→6)-linkages. GTFs activated NF-κB/AP-1 through MyD88 and TRIF pathways. GTFs stimulated TLR3, 7 and 9 while ITFs activated TLR2 and TLR4. GTFs strongly inhibited TLR2 and TLR4, while ITFs did not inhibit any TLR. Molecular docking demonstrated interactions of fructans with TLR2, 3, and 4 in a structure dependent fashion. Moreover, ITFs and GTFs attenuated pro-inflammatory cytokine production of stimulated DCs. These findings demonstrate immunomodulatory effects of GTFs via TLRs and attenuation of cytokine production in dendritic cells by GTFs and long-chain ITF.

1. Introduction

Economic progress has led to spreading of the Western life style which has contributed to an increased risk for development of non-communicable diseases such as cardiovascular diseases, stroke, cancer, diabetes and respiratory diseases (Beaglehole et al., 2011; Patry & Nagler, 2021). These changes in lifestyle include less physical activity, higher intake of processed foods enriched with animal fats as well as lower intake of dietary fibers compared to more traditional diets (Health & Services, 2015; Temba et al., 2021). During recent years, especially enhanced intake of dietary fibers has been shown to be an effective strategy to reduce risk for developing chronic metabolic and immune diseases (Veronese et al., 2018). However, the mechanisms that underlie these health benefits are not completely understood. It has been shown that beneficial effects of dietary fiber intake might be associated with enhanced production of short-chain fatty acids (SCFAs) by intestinal microbiota (Van den Abbeele et al., 2021) but also other mechanisms such as direct interaction of dietary fibers with immune cells in the intestine have been suggested to be involved (Vogt et al., 2013).

An important family of dietary fibers are fructans which can be found in the cell wall of bacteria, fungi or in angiosperm plants (Flamm et al., 2001; Oerlemans et al., 2020; Pérez-López & Simpson, 2020). Fructans

Abbreviations: AP-1, activating-protein 1; DP, degree of polymerization; EU, endotoxin units; FLA-ST, flagellin from *S. typhimurium*; FSL-1, synthetic diacylated lipoprotein - TLR2/TLR6 ligand; GTF I, graminan-type fructan I; GTF II, graminan-type fructan II; G418, geneticin; HEK, human embryonic kidney cells; HPAEC, high performance anion exchange chromatography; HPSEC, high-pressure size exclusion chromatography; CL264, 2-(4-((6-amino-2-(butylamino)-8-hydroxy-9H_purin_9-yl) methyl)benzamido)acetic acid; ITF I, inulin-type fructan I; ITF II, inulin-type fructan II; LAL, limulus amebocyte lysate; MWD, molecular weight distribution; NF-κB, Nuclear factor kappa-light-chain-enhancer of activated B cells; ODN 2006, class B CpG synthetic oligonucleotide; Poly I:C, high molecular weight-synthetic analog of dsRNA; SEAP, Secreted Alkaline Phosphatase; ssRNA40/LyoVec, single-stranded GU-rich oligonucleotide complexed with the cationic lipid LyoVec™; THP1, Human monocytic cells; TLRs, Toll-like receptors.

* Corresponding author at: Immunoendocrinology, Division of Medical Biology, Department of Pathology and Medical Biology, University of Groningen and University Medical Center Groningen, Hanzeplein 1, 9700 RB Groningen, the Netherlands.
E-mail address: c.fernandez.lainez@umcg.nl (C. Fernández-Lainez).

https://doi.org/10.1016/j.carbpol.2021.118893
Received 31 July 2021; Received in revised form 25 October 2021; Accepted 11 November 2021
Available online 15 November 2021
This is an open access article under the CC BY license (http://creativecommons.org/licenses/by/4.0/).

are water soluble and energy-storing polysaccharides in plants (Van den Ende, 2013). Fructans are synthesized from glucose units to which a fructose unit is added. According to their composition, fructans are denoted as GF_n or F_n, where "G" corresponds to the terminal glucose unit, "F" corresponds to fructose, and "n" denotes the number of molecules that elongate the fructan chain (Roberfroid, 2005). Fructans are structurally diverse, and their composition depends on the metabolism present in the plant from which they are extracted (Versluys et al., 2018). Fructans can be classified in several groups according to the position of fructose carbon atoms that form the glycosidic bond for the elongation. Inulins are a type of fructans composed of β(2→1) bonds. These β(2→1) inulins have a linear structure and are different from the inulin neoseries that contain a glucose moiety between two fructose chains linked through β(2→1) bonds (Vijn & Smeekens, 1999). Another form of fructans are levans which are comprised of β(2→6) bonds and are also linear. Just like inulin, these levans also exist as neoseries containing a central sucrose molecule to which fructose chains are linked by β(2→6) bonds (Mancilla-Margalli & López, 2006; Vijn & Smeekens, 1999). These levans can be extracted from both bacteria and plants, where they have different biological functions (Young, et al. 2021). A third family of fructans are the graminans. These fructans consist of a mixture of both β(2→1) bonds and β(2→6) bonds and have a branched structure. All these fructans have a β-configuration of their chemical bonds which makes them mostly inaccessible to human digestive enzymes. Therefore, fructans are widely considered to be non-digestible carbohydrates (NDCs) (Roberfroid et al., 1998).

Graminan type fructans (GTFs) isolated from *Agave tequilana* (agave) are widely used in Latin America and recognized for their health benefits (López & Urías-Silvas, 2007). Because of these health benefits they have been applied as prebiotics in infant formula for newborns (López-Velázquez et al., 2015). Despite these recognized benefits, still there is poor knowledge about the effects of GTFs on immune health. On the other hand, inulin-type fructans (ITFs) are well recognized for their metabolic and immune health benefits (Vogt et al., 2013) and those isolated from *Cichorium intybus* (chicory), are widely used and consumed in Europe as food supplement. For some ITFs it has been shown that their beneficial effect on immune health occurs via binding to Toll-like receptors (TLRs) (Vogt et al., 2013). In humans, TLRs are a group of ten transmembrane proteins that participate in the immune response against pathogenic microorganisms (Abreu, 2010). Once TLRs recognize specific pathogenic molecules such as lipoproteins from bacterial cell wall or genetic material (RNA, DNA) signaling cascades are activated (Gay & Gangloff, 2007). These signaling cascades can follow either the Myeloid Differentiation primary-response protein 88 (MyD88) or the TIR domain-containing adaptor protein inducing IFN-β (TRIF) pathways for the production of inflammatory cytokines (Takeda & Akira, 2004). ITFs can activate TLRs and regulate inflammatory responses and effects are chain-length dependent (Bermudez-Brito et al., 2015). These immunomodulatory properties can be beneficial for gut and immune health as previously demonstrated in human studies (Bermudez-Brito et al., 2015; Kiewiet et al., 2021; Vogt et al., 2017).

We hypothesized that fructans from agave exert immunomodulation via TLRs, which might explain their health benefits. To determine this, we performed the current study in which we investigated the modulatory effect of GTFs on TLRs which was compared to that of ITFs of different chain lengths. Furthermore, as it is unknown for both GTFs and ITFs how and on which binding sites they interact with TLR we applied in silico docking studies to propose the specific binding sites of fructans on TLRs. This was performed on the TLRs that were most strongly regulated by fructans. Finally, the impact of these fructans on the cytokine responses from dendritic cells (DCs) was studied.

2. Materials and methods

2.1. Fructans

In order to study the effects of linear or branched structures of fructans on TLR signaling, two types of branched β(2→1) and β(2→6) linked graminan-type fructans were tested. One is a mixture of low DP chains (GTF I, Metlos™) and the other is a mixture of predominant higher DP (GTF II, Metlin™) fructan, both extracted from *Agave tequilana* Weber blue variety, were provided by Nekutli™, Guadalajara, México. These GTFs were studied and compared with two previously described linear β(2→1)-linked inulin-type fructans, ITF I (Frutafit™ CLR) and ITF II (Frutafit™TEX!). ITF I is short chain (DP range 3–10) and ITF II is long chain (DP range 10–60). Both β(2→1) fructans extracted from *Cichorium intybus* root, were provided by Sensus™ B. V., Roosendaal, The Netherlands (Vogt et al., 2013).

2.2. Chemical characterization of inulin and Graminan-type fructans

Chain length profile of GTF I and GTF II, as well as those of ITFs tested, were determined through HPAEC analysis, with a Dionex (Sunnyvale, CA, USA) Carbopac PA-1 column (2 × 250 mm) preceded by a Carbopac PA-1 guard column (2 × 25 mm). Samples were analyzed at a concentration of 50 μg/ml and introduced with a partial-loop injection of 10 μl. Carbohydrates were separated with a gradient elution: 0–400 mM NaOAc in 100 mM NaOH during 40 min, followed by a washing step of 5 min with 1 M NaOAc in 100 mM NaOH and column equilibration with 100 mM NaOH for 15 min. Pulsed amperometrics was used as detection system with a Dionex ISC5000 ED detector (Vogt et al., 2013). Data were acquired with Chromeleon software version 7.0 (Thermo Scientific, San Jose, CA, USA). Annotation of individual components present in GTF I and GTF II was accomplished by comparison of the elution profiles with the previously characterized ITFs (Vogt et al., 2013).

For determination of fructans MWD, HPSEC on an Ultimate 3000 HPLC system (Dionex) coupled to a Shodex RI-101 refractive index detector (Showa Denko, Tokyo, Japan) was used. For the analysis, 20 μl of sample (2.5 mg/ml) dissolved in water were injected at 55 °C. Three TSK-Gel columns connected in tandem (4000–3000–2500 SuperAW; 150 × 6 mm, Tosoh Bioscience, Tokyo, Japan), with the TSK Super AW-L guard column (35 × 4.6 mm, Tosoh Bioscience) were used and samples were eluted at 0.6 ml/min with $NaNO_3$ (0.2 M). Data were acquired with Chromeleon software version 7.0 (Thermo Scientific) and MWD was calculated by interpolation in a pullulan (Polymer Laboratories, Palo Alto, Ca, USA) standard curve in a range of 0.18–790 kDa.

2.3. Endotoxin measurement and removal

Endotoxin levels of all fructans were determined with the commercial Pierce LAL Chromogenic Endotoxin Quantitation Kit™ according to the manufacturer instructions. In case endotoxin levels were above 1 EU/ml, we applied the Pierce High-Capacity Endotoxin Removal Resin™. This resin decreased the endotoxin levels to less than 1 EU/ml (Table S1). These endotoxin concentrations have no influence on the studied cells (Lépine & de Vos, 2018; Vogt et al., 2013). Once fructans were endotoxin-free, they were freeze-dried and stored at −20 °C until use. To exclude any influence from possible endotoxin remnants, we additionally performed tests in which we added the fructans to the cells in the presence and absence of 100 μg/ml of the endotoxin-blocker polymyxin B (Invivogen, Toulouse, France). There were no significant differences between treated and non-treated cells (Fig. S1).

2.4. Reporter cell lines

THP1-XBlue™-MD2-CD14 human monocytes were used as reporter cell-line. This is a cell line which endogenously expresses all human

TLRs and has been genetically modified with the SEAP inducible reporter gene, under control of NF-κB and AP-1 promoters. It also has an extra insert for the expression of MD2 and CD14 accessory proteins which enhance TLR signaling (Cheng et al., 2019; Sahasrabudhe et al., 2018). Additionally, human embryonic kidney cells (HEK-Blue™) expressing either human TLRs 2, 3, 4, 5, 7, 8 or 9 were applied. Also, this cell-line has a SEAP reporter gene system. It is important to note that HEK-Blue™ TLR2 cell line, also expresses the TLRs 1 and 6. TLR2 forms active heterodimers with TLR1 and TLR6 (Sahasrabudhe et al., 2018). All these cell lines were acquired from Invivogen (Invivogen, Toulouse, France).

THP1-XBlue™-MD2-CD14 and HEK-Blue™ cell lines were cultured in RPMI-1640 medium with 2 mM glutamine and DMEM medium (Lonza, Basel, Switzerland), respectively. RPMI-1640 contained normocin 100 μg/ml (Invivogen, Toulouse, France) and DMEM medium penicillin/streptomycin 50 U/ml and 50 μg/ml. (Gibco, Leicestershire, UK). Both media were supplemented with 10% heat-inactivated fetal bovine serum (Sigma, St. Louis, MO, USA), sodium bicarbonate 1.5 g/l (Sigma, St. Louis, MO, USA) and sodium pyruvate 1 mM (Biowest, Nuaillé, France). Selection antibiotics (Invivogen, Toulouse, France) are indicated in Table S2. Cell lines were passaged twice a week and worked at 80% confluency, according to manufacturer's instructions.

2.5. TLR activation and inhibition assays with reporter cell lines

Assays for quantifying TLR activation were performed in THP1-XBlue™-MD2-CD14 and HEK-Blue™ cell lines by incubating 200 μl of the experimental sample in 96-well plates, at cell densities indicated in Table S2. This was done during 24 h at 37 °C, 5% CO_2, in presence of 0.5, 1 or 2 mg/ml of GTFs, as well as of ITFs at 2 mg/ml. These working concentrations were based on response curves from previous studies (Lépine & de Vos, 2018; Vogt et al., 2013).

Culture medium and agonists for each TLR, were included as positive and negative controls respectively (Table S2). TLR activation was determined by quantitation of SEAP secretion from the supernatant of cells which was diluted 1:10 with Quantiblue™ reagent (Invivogen, Toulouse, France). After incubation for 1 h at 37 °C, the change in absorbance was measured at 655 nm in a Bio-Rad™ Benchmark Plus microplate spectrophotometer reader (Bio-Rad Laboratories B.V, Veenendaal, Netherlands). Data were normalized relative to negative control, which were set to 1.

To assess whether fructans induce TLR signaling through the MyD88 or TRIF pathways, the synthetic peptides Pepinh-MYD™ and Pepinh-TRIF™ (Invivogen, Toulouse, France) were used. Pepinh-MYD™ and Pepinh-TRIF™ block these signaling pathways. THP1 -XBlue™-MD2-CD14 cells were pre-incubated with 50 μM of Pepinh-MYD™ or Pepinh-TRIF™ for 6 h at 37 °C, 5% CO_2. Afterwards the different fructans were added and cells were incubated during 24 h, followed by quantitation of SEAP production. The fold-change of NF-κB/AP-1 was calculated as mentioned above.

To assess the inhibitory effect of GTFs and ITFs on TLRs, HEK-Blue™ cells were pre-incubated for 1 h at 37 °C, 5% CO_2 with the fructans, followed by addition of the appropriate TLR ligands and incubation during 24 h. Next, SEAP production was determined as mentioned above. Positive controls were cells treated only with each individual TLR-specific agonist. The inhibition rate was calculated as the fold-change of NF-κB/AP-1 induction, compared to each specific TLR agonist positive control.

2.6. Prediction of fructans binding mode to TLRs by molecular docking

To predict the potential interaction sites of the different fructans with TLR2 or with TLR3 or with TLR4, molecular docking analyses were performed. We used the protein-small molecule docking web service, which is based on the docking software EADock DSS from the Molecular Modeling Group of the Swiss Institute of Bioinformatics, Lausanne, Switzerland (Grosdidier et al., 2011). For performing the docking analyses, TLRs were defined as protein targets and fructans were defined as ligands.

The crystallographic structure from human TLR2 in complex with Pam3CSK4 agonist available in the Protein Data Bank was used (PDB code 2Z7X) (Jin et al., 2007). The crystallographic structure of human TLR3 ligand binding domain was also applied (PDB code 2A0Z) (Bell et al., 2005). The crystallographic structure of TLR4 in complex with myeloid differentiation factor 2 (MD2) and lipopolysaccharide (LPS) agonist was also applied (PDB code 3FXI) (Park et al., 2009).

Since β(2→6) linkage is exclusive of GTFs, as a first approximation to determine potential interaction sites of these fructans with TLRs, we selected the simplest β(2→6) oligosaccharide found in GTFs, which is β-D-fructofuranosyl-(2→6)-β-D-fructofuranosyl α-D-glucopyranoside (6-kestose). Since ITFs only possess β(2→1) linkages, the fructan β-D-fructofuranosyl-(2→1)-β-D-fructofuranosyl α-D-glucopyranoside (1-kestose), was used to investigate whether it could have different binding sites to TLRs. Crystallographic structure of 1-kestose was extracted from Protein Data Bank and 6-kestose 3D-structure was obtained from its simplified molecular-input line-entry system (SMILES) notation deposited in PubChem data base (Table S3) (Berman et al., 2000; Kim et al., 2019).

Linear inulin and branched agavin, both constituted of GF_{10} series, were chosen as representative ligands of ITF II and GTF II, respectively (Table S4). Hereinafter called GF_{10}-inulin and GF_{10}-agavin. GF_{10}-inulin 3D-structure was obtained by modification of the PubChem structure (ID: 24763). Avogadro software version 1.2.0 was used for construction of the structure (Hanwell et al., 2012). GF_{10}-agavin structure was constructed based on the structure proposed by Mancilla-Margalli et al. (Mancilla-Margalli & López, 2006) by using the Optical Structure Recognition Software (OSRA) (Filippov & Nicklaus, 2009) and Avogadro software for structure refinement (Hanwell et al., 2012).

Prior to docking analyses, the energy of protein targets and ligands 3D-structures were minimized using Yasara minimization server or Avogadro (Filippov & Nicklaus, 2009; Hanwell et al., 2012; Krieger et al., 2009). The different protein-ligand models obtained from molecular docking, were evaluated and analyzed using UCSF Chimera software version 1.14 (Pettersen et al., 2004). The interaction measures and figures were generated with Pymol Molecular Graphics System version 2.3.5 Edu, Schrödinger, LLC (DeLano, 2002).

2.7. Stimulation of dendritic cells with agave and chicory fructans

Human dendritic cells (DCs) isolated from umbilical cord blood CD34+ progenitor cells (MatTek Corporation, Ashland, MA, USA), were used. DCs were defrosted and seeded in 96-well plates (3×10^5 cells/well), with maintenance culture medium containing cytokines (DC-MM; Mat Tek Corporation, Ashland, MA, USA), according to manufacturer's instructions. In order to get them attached to the wells DCs were incubated for 24 h at 37 °C and 5% CO_2 (normal conditions).

The influence of ITFs and GTFs on DCs cytokine release was investigated by incubating them for 48 h in the presence or absence of 500 μg/ml of ITFs and GTFs dissolved in DCs maintenance culture medium. In order to test the inhibitory effect of fructans on immune cells, DCs were pre-incubated for 1 h with 500 μg/ml of ITFs and GTFs, followed by the addition of TLR4 agonist (LPS), and a mixture of TLR2 agonists (FSL-1 and Pam3CSK4) at 10 ng/ml. Afterwards, DCs were incubated in presence of the agonists during 48 h under normal conditions. Cell supernatants were collected and stored at −80 °C until further use. Positive controls were DCs treated only with TLR4 and TLR2 agonists. Untreated controls were cells cultured only with DCs culture medium. The inhibition rate was calculated as the fold-change of cytokines production, compared to each TLR agonist positive control.

2.8. Determination of cytokine profile

Magnetic Luminex ® Assay (R&D systems, Biotechne, Minneapolis, USA) was used to quantify the DCs cytokine profile (MCP-1/CCL2, MIP-1α/CCL3, IL-1RA, IL-1β, IL-6, TNFα and IL-10). The manufacturer's protocol was followed. Briefly, 50 μl of DCs supernatants or standard solutions were mixed in 96-well plates with a mixture of magnetic beads containing antibodies for the different cytokines. The plates were incubated overnight at 4 °C under constant shaking. Afterwards, detection antibodies were added and the plate was incubated at RT for 30 min under constant shaking. Later, the plate was washed three times, followed by incubation with streptavidin for 30 min at RT under constant shaking. Then, after three-wash steps in which 100 μl of wash buffer was added per well, the plate was read in a Luminex 200 system. The data were analyzed with the Luminex xPOTENT software. At least five independent assays were performed for each test.

2.9. Statistical analyses

Data were analyzed with GraphPad Prism™ software (version 8.2.1 for Windows™, San Diego, CA, USA). Normal distribution of data was assessed with Shapiro-Wilk test. Normal distributed data were analyzed with one-way ANOVA followed by Dunnett's multiple comparisons adjustment. Non-parametric distributed data was analyzed with Mann-Whitney *U* test or Friedman test, followed by Dunn's multiple comparisons adjustment test. Results are expressed as mean ± SD or as median and interquartile range (IQR), for data with parametric and non-parametric distribution respectively. A p-value <0.05 was considered to be statistically significant ($^{*}p < 0.05$, $^{**}p < 0.01$, $^{***}p < 0.001$, $^{****}p < 0.0001$), p-values < 0.1 were considered as a trend.

3. Results

3.1. Characterization of inulin and graminan-type fructans

Inulin and graminan-type fructans were analyzed for determination of their molecular weight distribution profiles and the components that make up the mixtures. ITFs are inulin-type fructans with only β(2→1) linkages (Vogt et al., 2013). The DP of ITF I ranges from 3 to 10 (Fig. 1 a), but it also has chains with DP up to 25. These fructan is a fructooligosaccharide-enriched inulin, containing both GF_n and F_n type oligosaccharides, although the GF_n series is the most dominant over the F_n series in this fructan (Fig. 1b). ITF II consists only of GF_n units, with a broad range of chain lengths from DP9 to 60 (Fig. 1b). GTFs are a mixture of oligosaccharides linked by β(2→1) and β(2→6) (Lopez et al., 2003). DP 3 and 4 make up most of the GTF I mixture, although it has a very low amount of components in the range of DP 7–45 (Fig. 1a). GTFs contain F_n type oligosaccharides as well as GF_n series. The oligomer

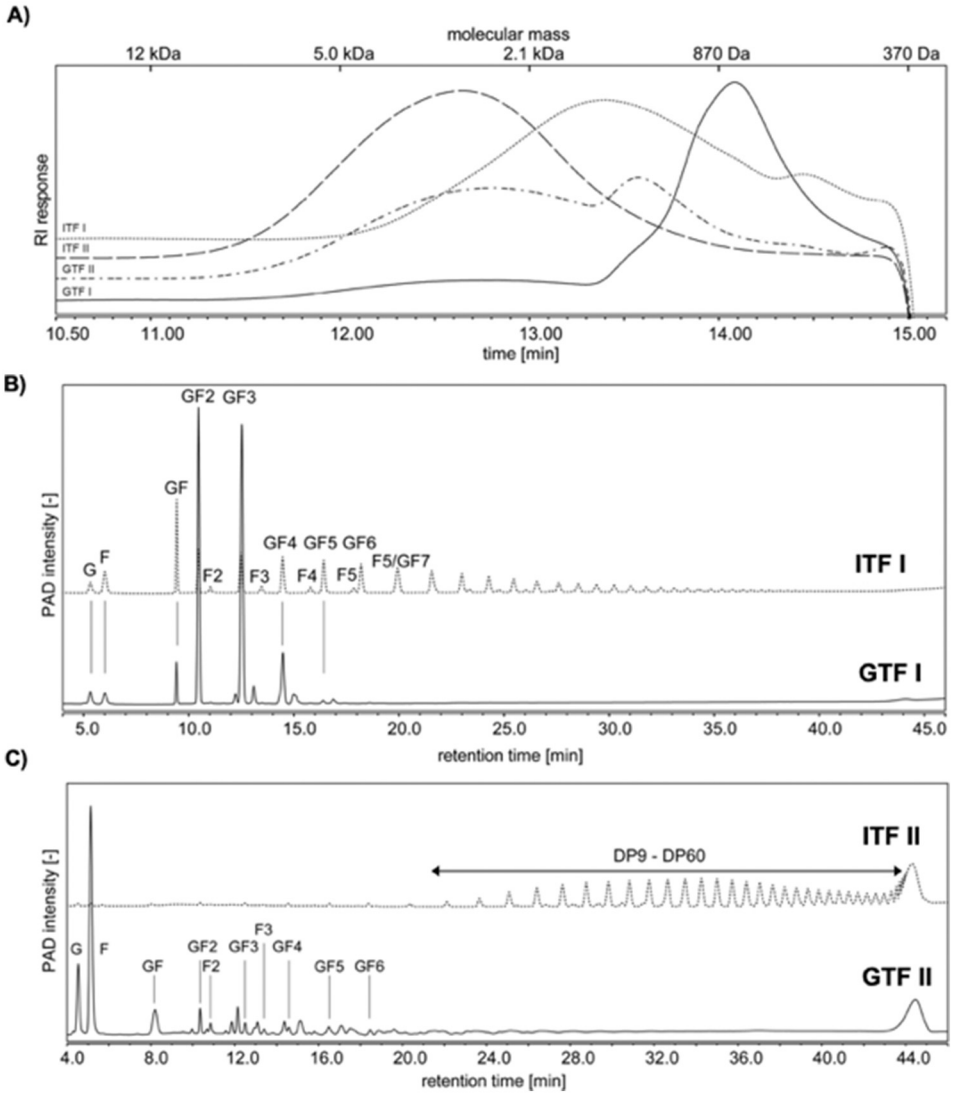

Fig. 1. HPSEC and HPAEC profiles of fructans from *Agave tequilana* and *Cychorium intybus*. (A) Molecular weight distribution profiles of ITFs and GTFs. GTF I molecular weight distribution is DP 3–4. ITF I has chains smaller than 10 DP. GTF II DP is around 17 with the presence of high molecular weight components. ITF II DP ranges between 9 and 60. Calibration of the system using pullulan standards is indicated. B) GTF I is composed of fructofuranosyl units with a terminal glucose. C) GTF II components belong to the GF series as well, and some others are of the Fn series. ITF II consists only of fructans of the GF_n type.

profile obtained from HPAEC demonstrates that GTF I is mainly composed of kestose (GF_2), nystose (GF_3) and fructosylnystose (GF_4) (Fig. 1b). GTFII contains in addition to these sugars, oligosaccharides F_2 and F_3 (Fig. 1c). GTF II has longer structures of which DP17 is the most abundant. Furthermore, in both GTFs, but specially in GTF I peaks that overlap with those of ITFs were detected. Additionally, in these studied GTFs, there were peaks detected which did not overlap with the ITFs profiles and hence, might represent the (neo-) levan or graminan type fructans.

3.2. GTFs are stronger stimulators of NF-kB activation in THP-1-MD2-CD14 cells than ITFs

ITFs and GTFs were tested for their capacity to induce NF-κB/AP-1 activation in a THP1-MD2-CD14 reporter cell line, which endogenously expresses all TLRs. NF-κB and AP-1 are essential transcription factors in signaling for cytokine release. ITFs were tested at a concentration of 2 mg/ml, as this was shown in a previous study to be an effective dose (Lépine & de Vos, 2018; Vogt et al., 2013). GTFs were tested at concentrations of 0.5, 1, and 2 mg/ml, as the concentration-dependent effects are unknown.

None of the ITFs were found to activate NF-κB/AP-1, except for ITF I in presence of MyD88 inhibitor (Fig. 2). This was different with GTF I and II that both activated NF-κB/AP-1. GTF I stimulated NF-κB/AP-1 only very mildly and only at a low concentration of 1 mg/ml (Fig. 2a). This was different with GTF II, as the fold change was of 1.59 ($p < 0.001$) compared with controls, and gradually increased with higher doses (Fig. 2b). Next, we determined whether the NF-κB/AP-1 activation observed with GTF I and II depends on the MyD88 signaling pathway, by repeating the experiments and adding the MyD88 inhibitor at 50 μM. MyD88 is the central transcription factor for all TLRs, with exception of TLR3 and endosomal TLR4. This MyD88 suppression resulted in complete loss of GTF I activation but, the effect was not MyD88-dependent with GTF II, as no reduction of NF-κB/AP-1 induced activation was observed in presence of Pepinh-MYD (Fig. 2c–d). As TLRs might also signal via TRIF pathway, we repeated the experiments with the TRIF inhibitor peptide, and also tested GTF I during TRIF inhibition. This resulted in a complete blockade of the GTF II induced activation of NF-κB/AP-1, and had no effect on GTF I (Fig. 2e–f).

3.3. TLR-activation is fructan type-dependent

The foregoing experiments demonstrate that the activating effect of GTFs and to a lesser extent the activating capacity of ITFs, are TLR dependent either via MyD88 or TRIF signaling. To identify which TLRs are activated, GTFs were also tested on reporter HEK-Blue cell lines which express either TLRs 2, 3, 4, 5, 7, 8 or 9. GTFs were tested at concentrations of 0.5, 1, and 2 mg/ml, while ITF I and II were included to allow comparison between β(2→1) and β(2→1)-β(2→6) fructans. To this end, we compared ITF I with GTF I as they are similar mixtures of chain-length values and we compared ITF II with GTF II because they share components with DP higher than 60.

ITF I only activated TLRs 2, 4 and 9. It exerted a stronger activation of TLRs 2 and 4, than of TLR 9 (Fig. 3a, c, g). Values were different with GTF I, which stimulated all TLRs. ITF I exerted a stronger activation of TLR2, which was 3.2 ($p < 0.0001$) fold enhanced and only 1.2 with GTF I ($p < 0.001$) (Fig. 3a). Also, TLR4 was strongly stimulated with ITF I which was 2.57-fold enhanced ($p < 0.0001$), and only 1.08-fold by GTF I (Fig. 3c). Effect on TLR5 by both fructans was similar and low, as it only induced a fold change of 1.05 for ITF I and 1.2 ($p < 0.05$) for GTF I (Fig. 3d).

ITF II only slightly stimulated TLRs 2 and 4 (Fig. 3h, j). While GTF II activated all TLRs in a dose-dependent manner, except on TLR4. The strongest stimulation observed with GTF II was on TLR9, with a 5.4-fold change ($p < 0.0001$), which was of 1.09 with ITF II (Fig. 3n). Also, GTF II induced a 4.05 ($p < 0.0001$) fold enhancement of TLR3 (Fig. 3i), which was of 1.04 with ITF II. Between GTF II and ITF II, a low and similar activating effect was observed on TLR4, which was 1.19 enhanced by GTF II, and 1.28 enhanced by ITF II ($p < 0.01$) (Fig. 3j).

3.4. Fructan-type influence the magnitude of inhibitory effect on individual TLRs

As the final effects of fructans on THP-1-MD2-CD14 cells may depend on the sum of activating and inhibiting effects of the fructans, we also studied and compared inhibitory effects of ITFs and GTFs on TLRs. To this end, all HEK-Blue™ cells were pre-incubated for 1 h with either 2 mg/ml of linear or 0.5, 1 and 2 mg/ml of branched fructans, followed by administration of the appropriate agonists to each cell line.

ITF I suppressed TLR5 and 9, with a fold change of 0.78 ($p < 0.001$) for TLR5 (Fig. 4c), and a fold change of 0.9 ($p < 0.0001$) for TLR9 (Fig. 4f). The other TLRs were unaffected by ITF I (Fig. 4). This was different with GTF I which strongly inhibited the activation of TLR 4, 8 and 9 in a dose dependent way (Fig. 4b, e, f). TLR4 activation was strongly inhibited by GTF I from 0.834 ($p < 0.0001$) to a 0.0.395-fold reduction ($p < 0.0001$), while the activation of TLR4 was not affected by ITF I (Fig. 4b). TLR9-activation was reduced from 1.006 to a fold change of 0.75 ($p < 0.0001$) by GTF I, while it was reduced to 0.9 ($p < 0.0001$) with ITF I (Fig. 4f). Interestingly, increasing the concentration of GTF I, did not inhibit but rather significantly enhanced TLR3 and 7 activation (both $p < 0.0001$), which did not occur with ITF I (Fig. 4a, d).

As TLR2 forms heterodimers with TLR1 and TLR6 to induce immune responses, we separately tested inhibition of TLR2-TLR1 by using the specific agonist Pam3CSK4, and for TLR2-TLR6 heterodimer by applying FSL-1. As shown in Fig. 5 a and c, the strongest inhibitory effect exerted by GTF I, was observed on TLR2-TLR6 activation, which was reduced from a fold change of 0.798 ($p < 0.05$) to 0.317 ($p < 0.0001$), and for TLR2-TLR1 the signaling was reduced from a fold change of 0.899 ($p < 0.05$) for 0.5 mg/ml of GTF I, to a fold change of 0.409 ($p < 0.0001$) for 2 mg/ml of GTF I. The activation of TLR2 was not inhibited by ITF I.

ITF II had no inhibitory effect on TLRs-activation, while GTF II strongly inhibited TLR2, 4 and 9 in a dose-dependent manner (Figs. 5b, d, 6b, f). TLR4 activation was strongly inhibited by GTF II, and such effect was proportional as the concentration increased, from a fold-change of 0.867 ($p < 0.001$) to 0.565 ($p < 0.001$) (Fig. 6b). To a lesser extent, GTF II inhibited TLR9 activation from 0.979 to a fold-change of 0.88 ($p < 0.0001$) (Fig. 6f).

In addition, the branched GTF II strongly inhibited TLR2-TLR1 activation in a dose-dependent way (Fig. 5b). This was mainly due to a strong reduction from 0.897 to a fold change of 0.421 ($p < 0.0001$). While the TLR2-TLR6 activation was reduced from 0.861 to 0.395 ($p < 0.0001$) with GTF II 0.5 mg/ml and 2 mg/ml respectively (Fig. 5d).

Instead of being inhibited, TLR3, 5, 7 and 8 were significantly increased with higher doses of GTF II. The largest increase observed was for TLR3 with a fold change of 2.1 ($p < 0.001$). This was not observed when cells were pre-treated with ITF II (Fig. 6a, c, d, e).

3.5. Docking predicts fructans bind differently to TLRs

In order to gain insight into the molecular mechanisms that drive the different activation and inhibitory effects exerted by ITFs and GTFs on TLRs, molecular docking analyses were performed. To that end, 1-kestose, 6-kestose, GF_{10}-inulin and GF_{10}-agavin were selected as one of the simplest structures that are present in the different fructans studied. From the aforementioned structures, ITF I can only have 1-kestose, GTF I and GTF II can have 6-kestose but neither of the ITFs can have it. ITF II can only have GF_{10}-inulin but cannot have GF_{10}-agavin, and GTF II can have both GF_{10}-inulin and GF_{10}-agavin. TLR2, TLR4 and TLR3 were chosen for these analyses as they were strongly influenced by the fructans and also because their crystal structure is well known.

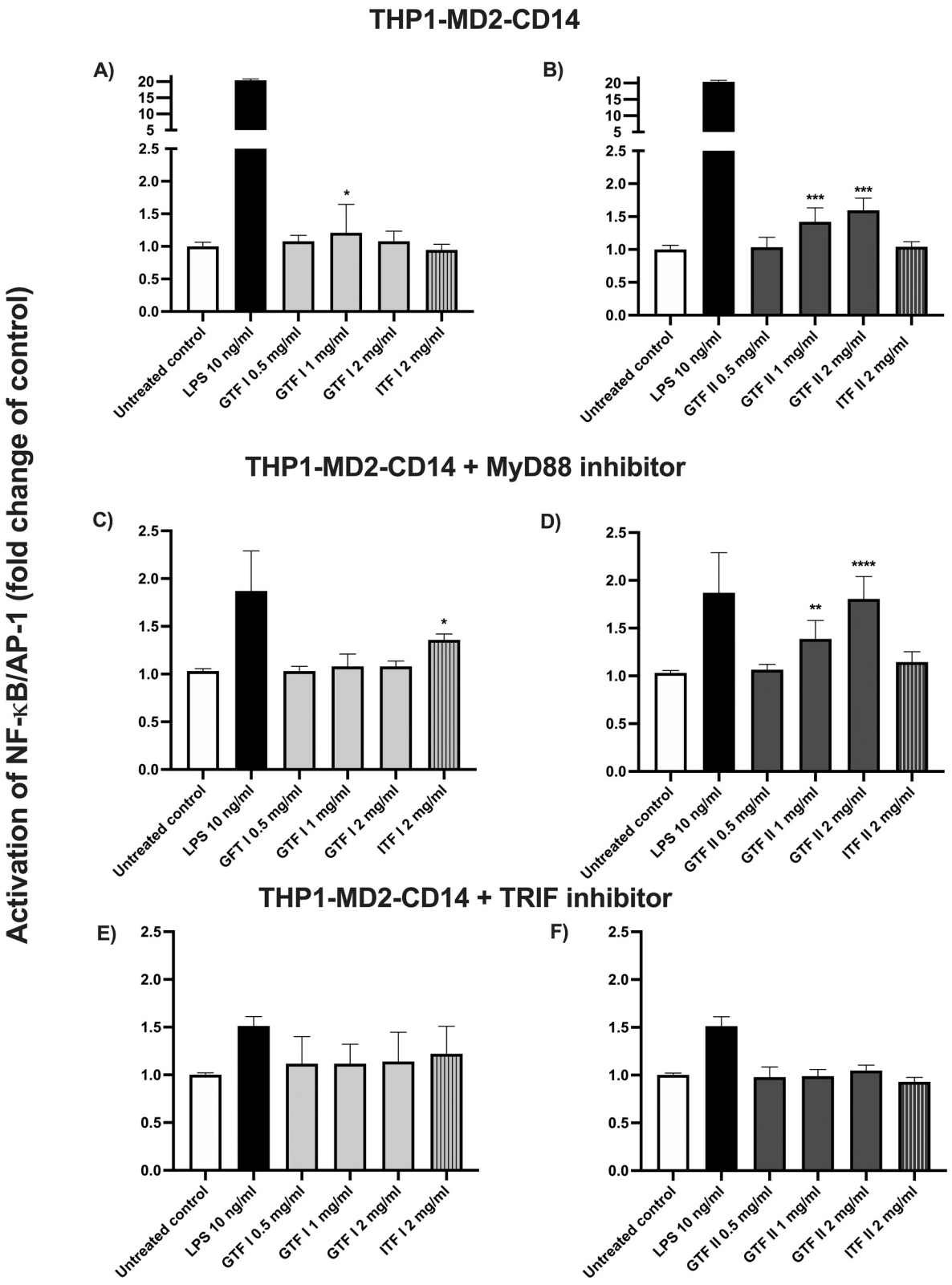

Fig. 2. NF-κB/AP-1 activation in THP1-MD2-CD14 reporter cells expressing all TLRs. A–B) THP1-MD2-CD14 cells. C–D) THP1-MD2-CD14 cells with Pepinh-MYD. E–F) THP1-MD2-CD14 cells with Pepinh-TRIF. Cells were pre-incubated in presence and absence of MyD88 inhibitor Pepinh-MYD, or TRIF inhibitor Pepinh-TRIF during 6 h before stimulation with 2 mg/ml of short and long linear chain fructans (ITF I and II) and 0.5, 1 and 2 mg/ml of short and long branched chain fructans (GTF I and II), after 24 h of incubation, NF-κB/AP-1 release was determined. Activation of NF-κB/AP-1 is presented as fold change of the untreated control. Results represent the median with interquartile range of at least three independent experiments, with three technical replicates. Statistical significance levels compared to the negative control were determined by Friedman test (non-parametric statistical test), followed by the Dunn's multiple comparisons test (post hoc test). A p-value <0.05 was considered to be statistically significant ($^{*}p < 0.05$, $^{**}p < 0.01$, $^{***}p < 0.001$, $^{****}p < 0.0001$), p-values < 0.1 were considered as a trend.

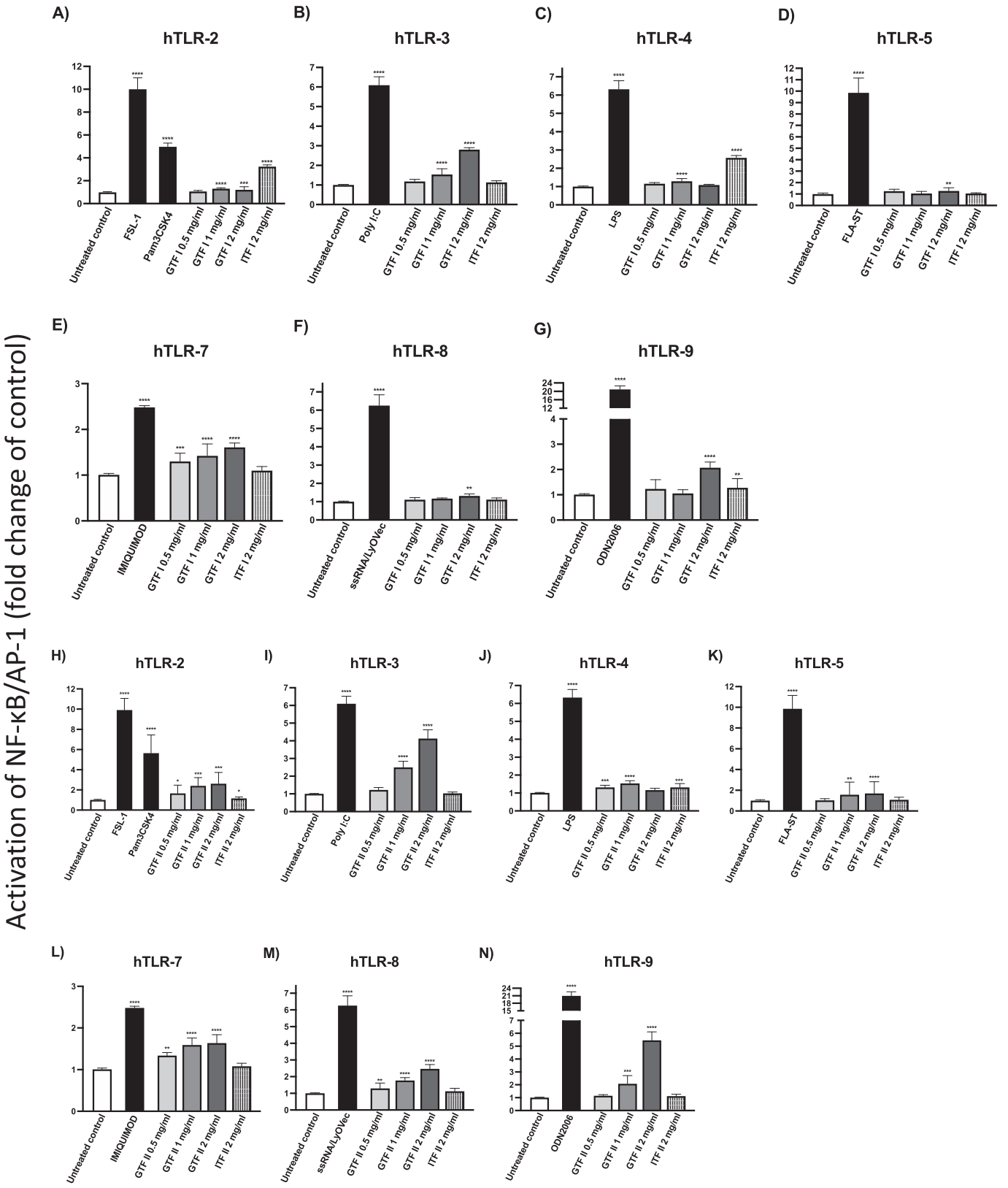

Fig. 3. Activation effects of ITFs and GTFs on HEK-Blue™ reporter cell lines. Each cell line was incubated during 24 h with 2 mg/ml of ITFs and 0.5, 1 and 2 mg/ml of GTFs. Next, NF-κB/AP-1 release was determined. Activation of NF-κB/AP-1 is presented as fold change of the untreated control. A–G) NF-κB/AP-1 activation effect of GTF I compared with ITF I. H–N) NF-κB/AP-1 activation effect of GTF II compared with ITF II. Appropriate agonists for each TLR served as positive controls. At least five independent assays, each one with three technical replicates. These data were normally distributed. Therefore, results are represented as the mean ± SD. Statistical significance levels compared to the negative control were determined by one-way ANOVA with Holm-Sidak's multiple comparisons test. A p-value <0.05 was considered to be statistically significant (*$p < 0.05$, **$p < 0.01$, ***$p < 0.001$, ****$p < 0.0001$), p-values < 0.1 were considered as a trend.

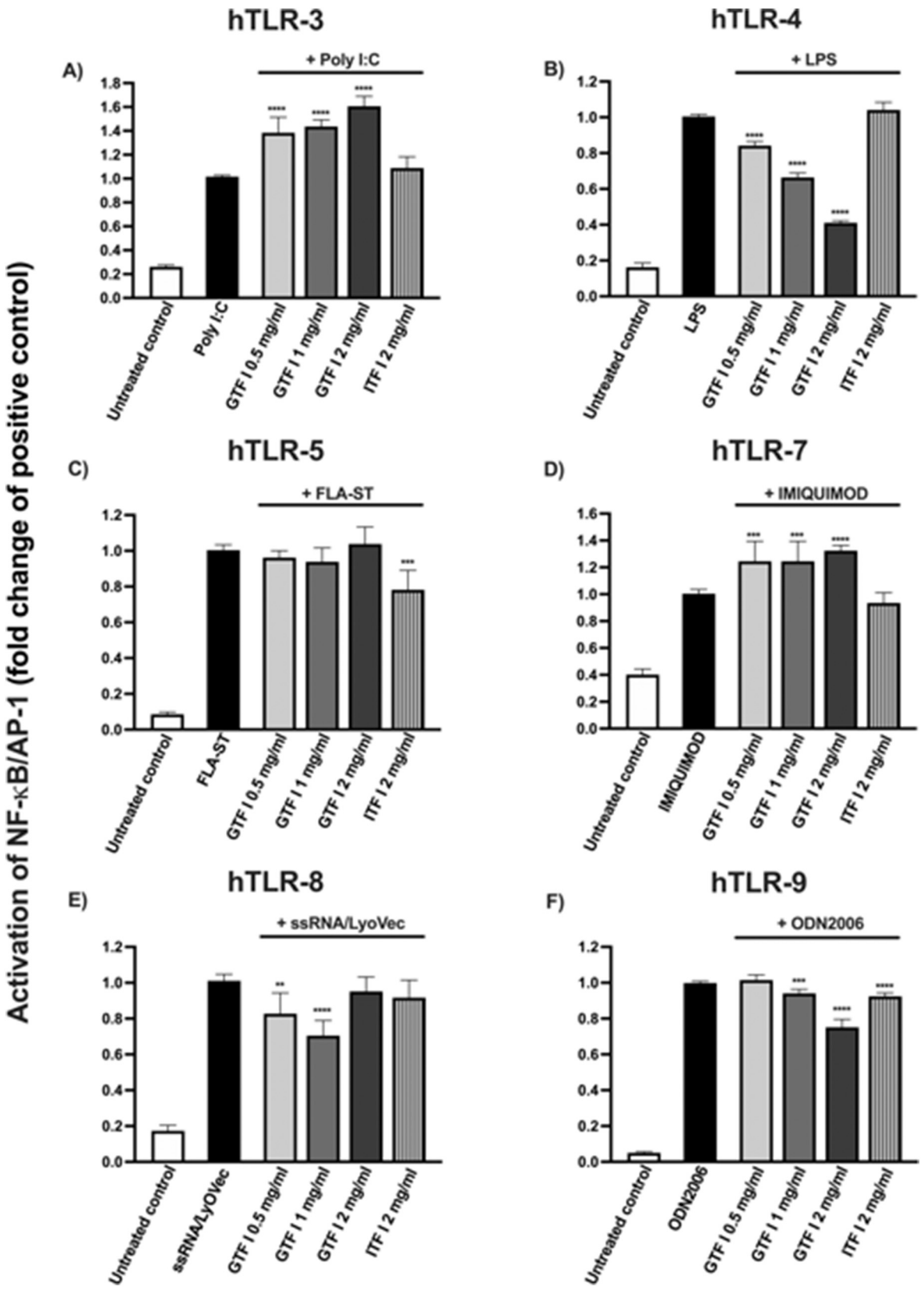

Fig. 4. Inhibitory effects of ITF I and GTF I on HEK-Blue™ reporter cell lines. Cells expressing TLR3 (A), TLR4 (B), TLR5 (C), TLR7 (D), TLR8 (E), and TLR9 (F), were pre-incubated during 1 h with short linear ITF I at 2 mg/ml and short branched GTF I at 0.5, 1 and 2 mg/ml, followed by the addition of the specific agonists for each TLR, and incubation of 24 h. Next, NF-κB/AP-1 release was determined. Panels A-F show inhibitory effect of GTF I and ITF I on TLRs activation, expressed as fold-change of NF-κB/AP-1 induction, compared to that of each specific TLR agonist. Results represent the mean ± SD of at least five independent assays, each with three technical replicates. Statistical comparisons were performed with one-way ANOVA and Geisser-Greenhouse correction, followed by Dunnett's multiple comparisons test. A p-value <0.05 was considered to be statistically significant (*$p < 0.05$, **$p < 0.01$, ***$p < 0.001$, ****$p < 0.0001$), p-values < 0.1 were considered as a trend.

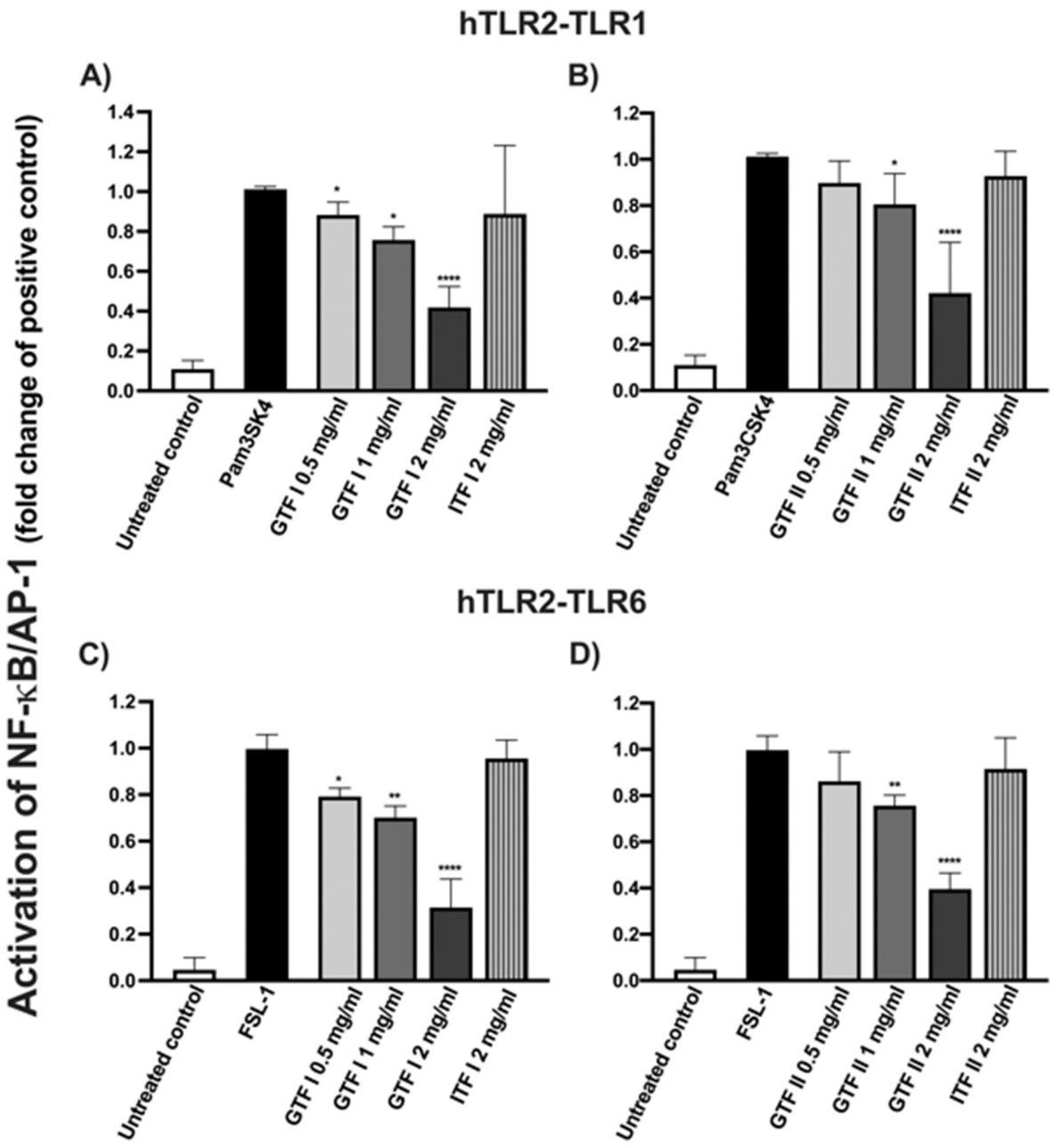

Fig. 5. Inhibitory effects of GTFs on HEK-Blue™ hTLR2 cells. Cells expressing TLR2-1 and TLR2-6 heterodimers, were pre-incubated during 1 h with 2 mg/ml of ITF I and ITF II, and 0.5, 1 and 2 mg/ml of GTF I and GTF II, followed by addition of the specific agonists Pam3CSK4 for TLR2-TLR1 heterodimer, and FSL-1 for TLR2-TLR6 heterodimer. After 24 h of incubation, NF-κB/AP-1 release was determined. Panels A–B show inhibitory effects of fructans on TLR2-TLR1 heterodimer activation, and panels C–D show inhibitory effect of fructans on TLR2-TLR6 heterodimer activation, expressed as fold-change of NF-κB/AP-1 induction, and compared to the positive control of each TLR2-heterodimer. Results represent the mean ± SD of at least five independent assays, each with three technical replicates. Statistical comparisons were performed with one-way ANOVA and Geisser-Greenhouse correction, followed by Dunnett's multiple comparisons test. A p-value <0.05 was considered to be statistically significant (*$p < 0.05$, **$p < 0.01$, ***$p < 0.001$, ****$p < 0.0001$), p-values < 0.1 were considered as a trend.

3.5.1. TLR2 docking predicted interactions

Molecular docking analysis of TLR2 with representative molecules of fructans, located them in different sites of this receptor. The best ranked pose of 1-kestose had a binding energy of −9.85 kcal/mol. 1-kestose established interactions with TLR2 residues at the central part of the ectodomain. Polar residues from TLR2 such as R447, S445 and K422 were interacting with 1-kestose (Fig. 7a–c). This was different with 6-kestose. The best ranked pose of 6-kestose had a binding energy of −8,22 kcal/mol and was found in a different region than the one found for 1-kestose. 6-kestose was located within the agonist binding pocket of TLR2. 6-kestose interacted with the 18 residues that conforms the pocket [27]. Most of amino acid residues interacting with 6-kestose were non-polar, such as leucine, isoleucine and valine. Three hydrogen bonds were formed between F322, F349 and L350 residues and 6-kestose (Fig. 7d–e).

1-kestose was found at the surface of TLR2 at the central ectodomain and at 19.2 Å from the entrance of the agonist binding site. GF_{10}-inulin was interacting with amino acid residues H238, L214, T236, Q209, D233 and K208 through hydrophobic interactions and hydrogen bonds (Fig. 7f–h).

GF_{10}-agavin was found located outside of the TLR2 pocket agonist entrance, exerting a partial blocking of this cavity, it was found

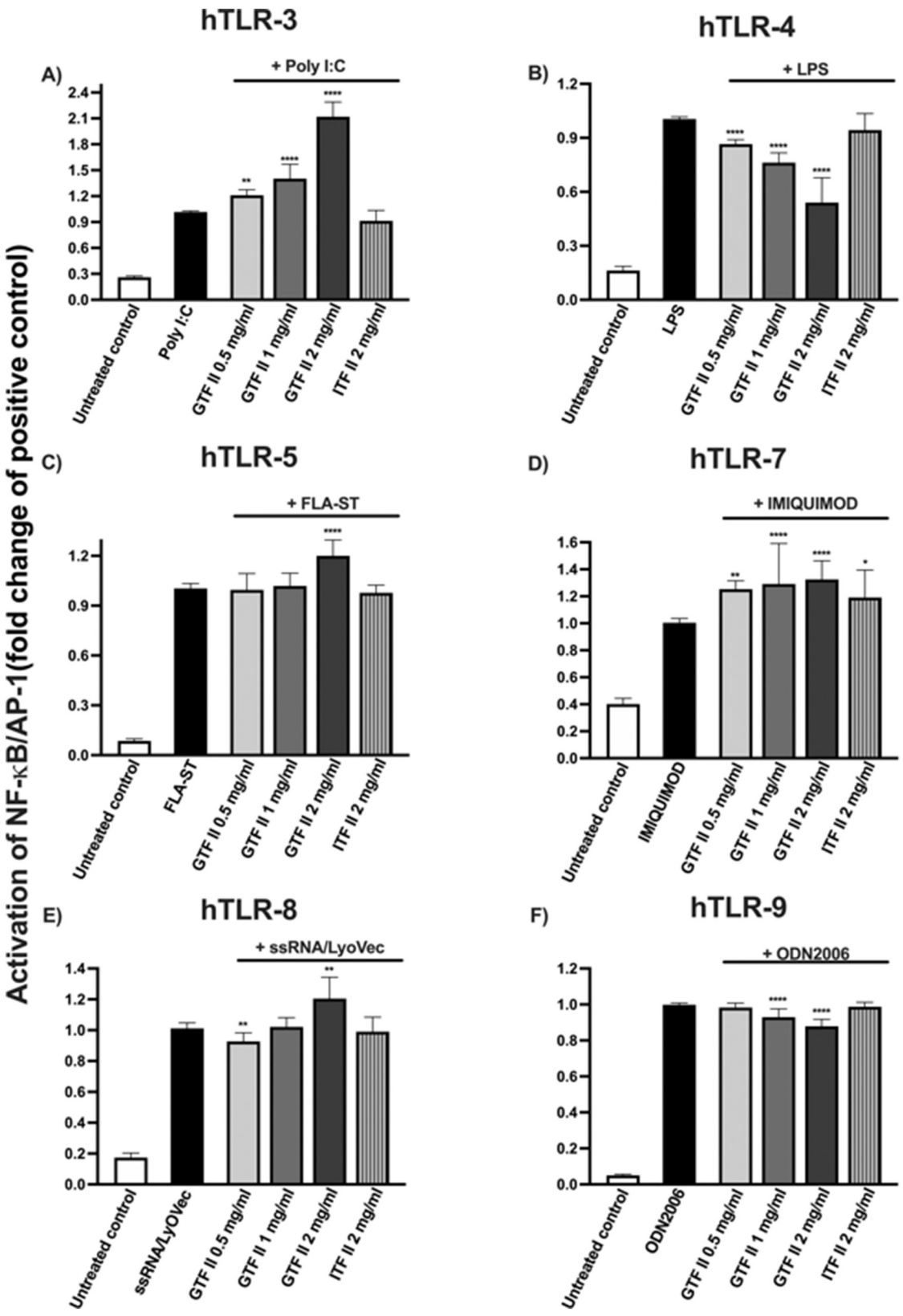

Fig. 6. Inhibitory effects of ITF II and GTF II on HEK-Blue™ reporter cell lines. Cells expressing TLR3 (A), TLR4 (B), TLR5 (C), TLR7 (D), TLR8 (E), and TLR9 (F), were pre-incubated during 1 h with ITF II at 2 mg/ml and GTF II at 0.5, 1 and 2 mg/ml, followed by the addition of the specific agonists for each TLR, and incubation of 24 h. Next, NF-κB/AP-1 release was determined. Panels A–F show inhibitory effect of GTF II and ITF II on TLRs activation, expressed as fold-change of NF-κB/AP-1 induction, compared to that of each specific TLR agonist. Results represent the mean ± SD of at least five independent assays, each with three technical replicates. Statistical comparisons were performed with one-way ANOVA and Geisser-Greenhouse correction, followed by Dunnett's multiple comparisons test. A p-value <0.05 was considered to be statistically significant ($^{*}p < 0.05$, $^{**}p < 0.01$, $^{***}p < 0.001$, $^{****}p < 0.0001$), p-values < 0.1 were considered as a trend.

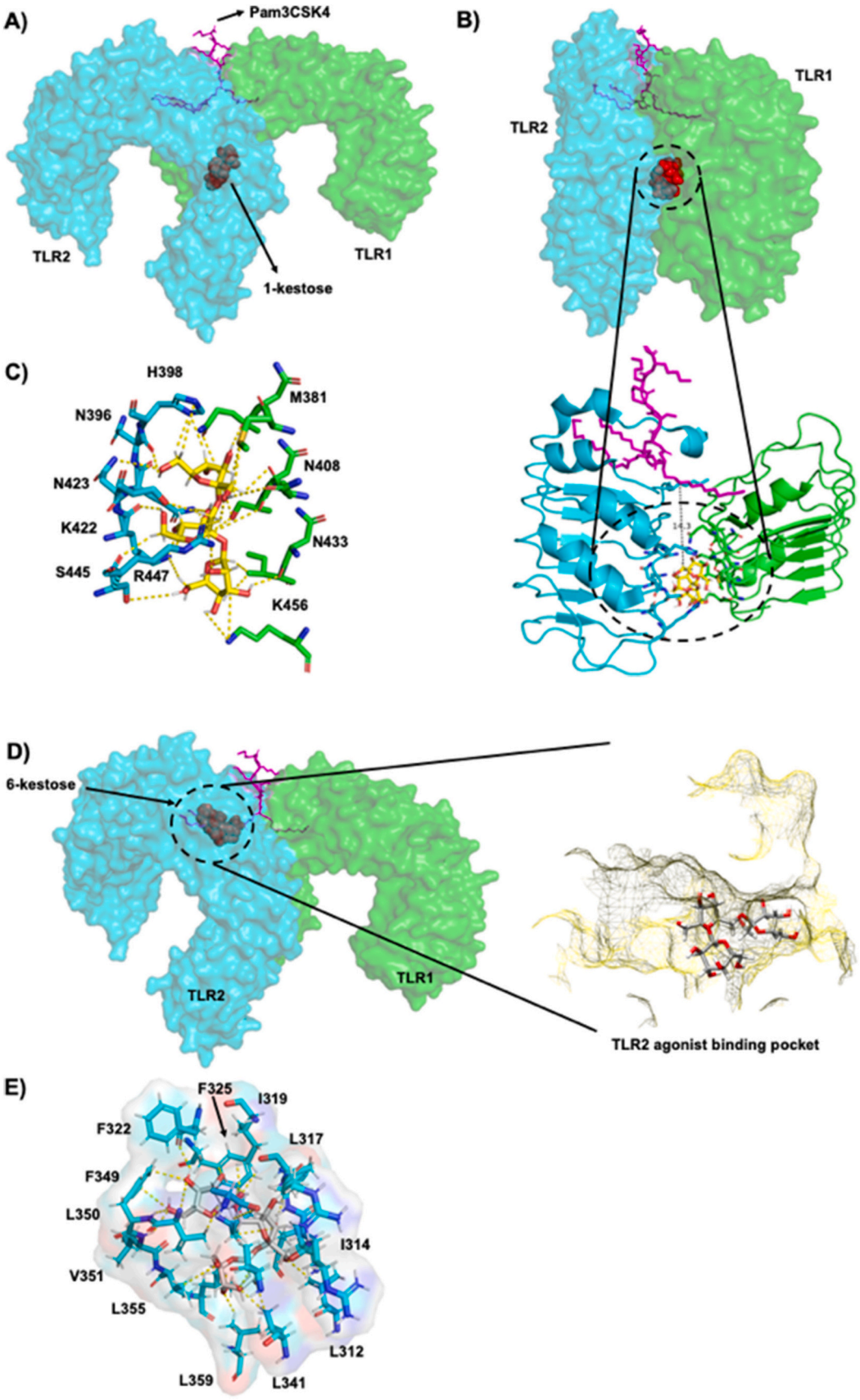

Fig. 7. Proposed binding site of fructans to TLR2-TLR1. Panels A–C demonstrates that 1-kestose binds to residues of the TLR2-TLR1 interface. Panels D–E indicates that 6-kestose has affinity to the Pam3CSK4 binding pocket of TLR2-TLR1. Panels F–H shows that GF_{10}-inulin interacts with the TLR2 surface. Panels I–J show GF_{10}-agavin established molecular interactions with amino acid residues of the agonist entrance pocket.

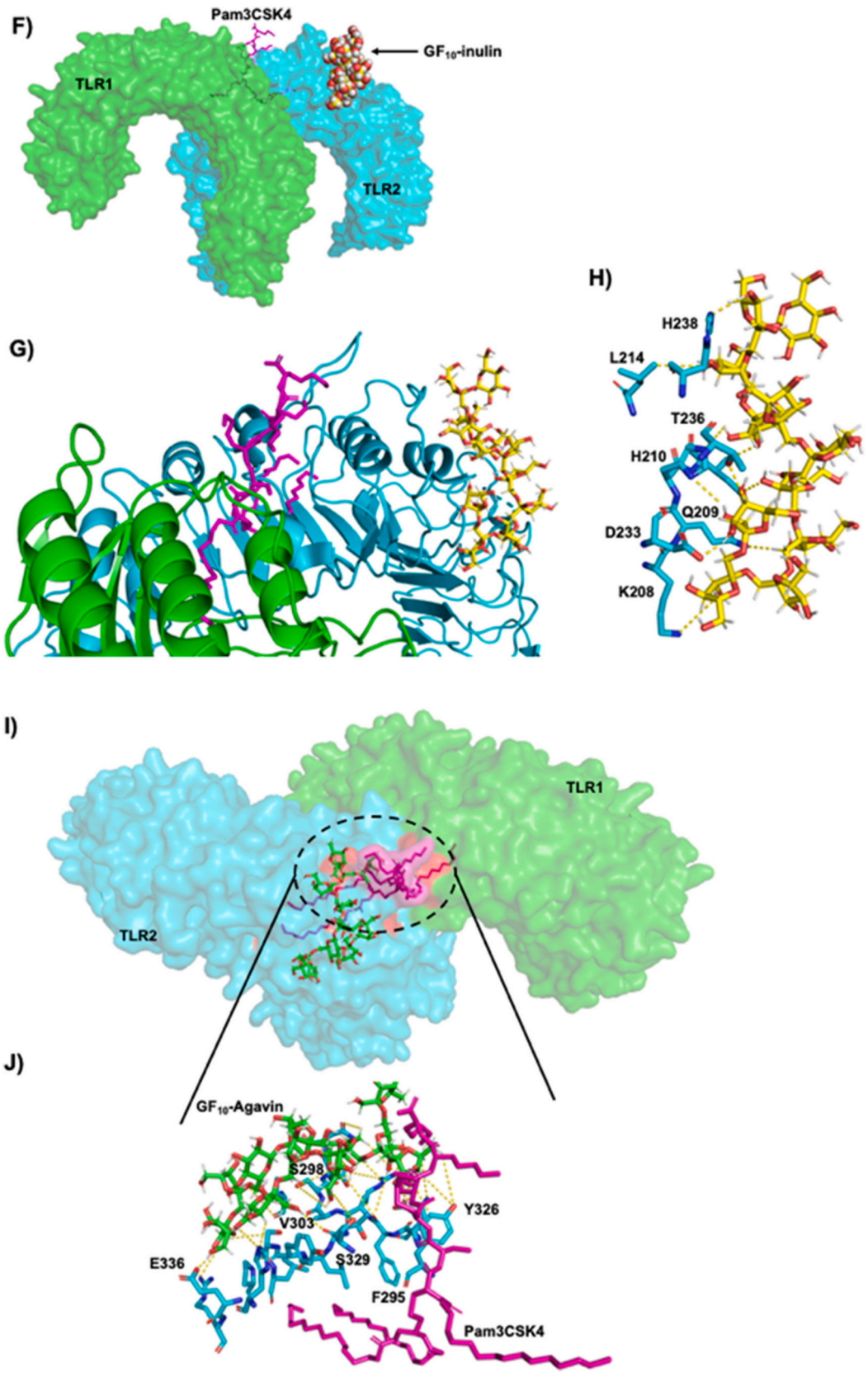

Fig. 7. (*continued*).

interacting with key amino acid residues of the binding site, such as Y326 and F325 (Fig. 7i–j).

3.5.2. TLR4 docking predicted interactions

As profound TLR4 inhibitory effects were observed for GTFs, docking analysis was performed to predict the potential binding sites of these

fructans. Docking analysis was made with the TLR4-MD2 complex with each of the four fructans. The functional unit of the TLR4-MD2 complex is formed by two TLR4 subunits, each forming a heterodimer with one MD-2 protein (Fig. 8a). The analysis predicts 1-kestose to bind within the MD-2 protein pocket (Fig. 8a). 1-kestose was found to interact only with MD-2 protein mainly through hydrophobic interactions with non-polar amino acid residues, such as I52, L61, L78, F147 and F151 (Fig. 8b–c). 6-kestose was also found within the MD-2 pocket (Fig. 8f), however the hydrophobic residues I32, I46, I94 and Y102 interacted with 6-kestose but not with 1-kestose (Fig. 8e–f). GF_{10}-inulin was found near the TLR4-MD2 interface (Fig. 8g). GF_{10}-inulin only interacted with amino acid residues of TLR4 such as H458 and G384, and those residues have not been described as key residues for interaction with LPS or for heterodimerization (Fig. 8h–i). Conversely, GF_{10}-agavin was found to interact with TLR4 as well as with MD-2 (Fig. 8j). GF_{10}-agavin established contact with some of the MD2 amino acid residues that participate in the interaction with LPS such as I124. Furthermore, GF_{10}-agavin interacted with 14 amino acid residues from MD-2 (Fig. 8k–l).

3.5.3. TLR3 docking predicted interactions

Enhancement of the activation instead of inhibition of TLR3 mediated by GTFs was found during the inhibition assays (Figs. 4a, 6a). In order to gain insight in the possible mechanism, docking analyses were performed with TLR3 and representative molecules of fructans. 1-kestose was located at the non-glycosylated side face of TLR3 (Fig. 9a, b), interacting with polar amino acid residues of TLR3, such as S160, K187 and E190 (Fig. 9c). 6-kestose was found located at N-terminal end of TLR3 (Fig. 9d–e). This molecule was interacting with key amino acids

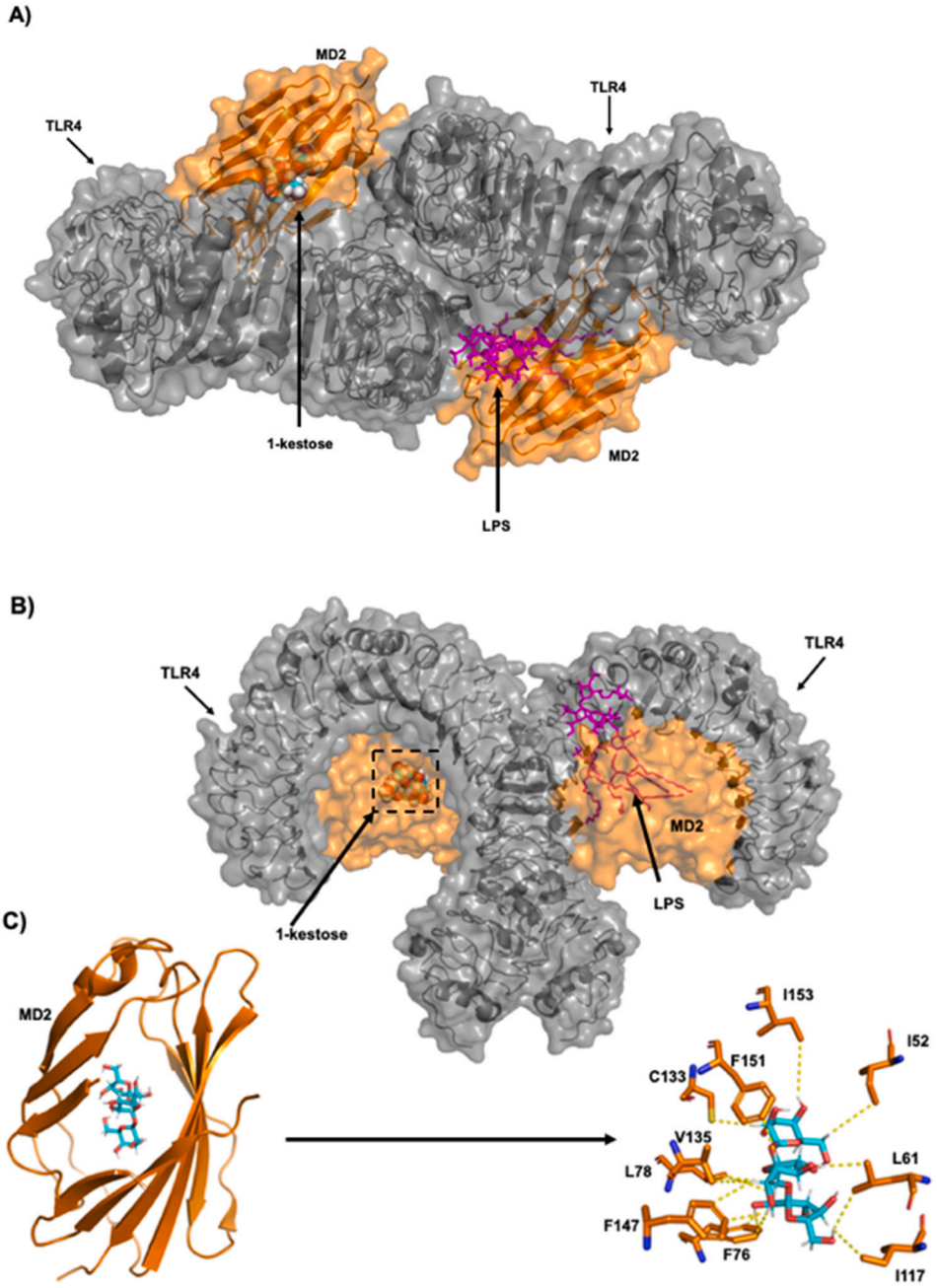

Fig. 8. Predicted sites of interaction between fructans and the TLR4-MD-2 heterodimer. The 1-kestose binding site was within the MD-2 pocket (A–C). 6-kestose established interactions with hydrophobic residues of the MD-2 pocket (D–F). GF_{10}-inulin only interacted with TLR4 amino acid residues (G–I). GF_{10}-agavin was found to interact with both TLR4 and MD-2 (J–L).

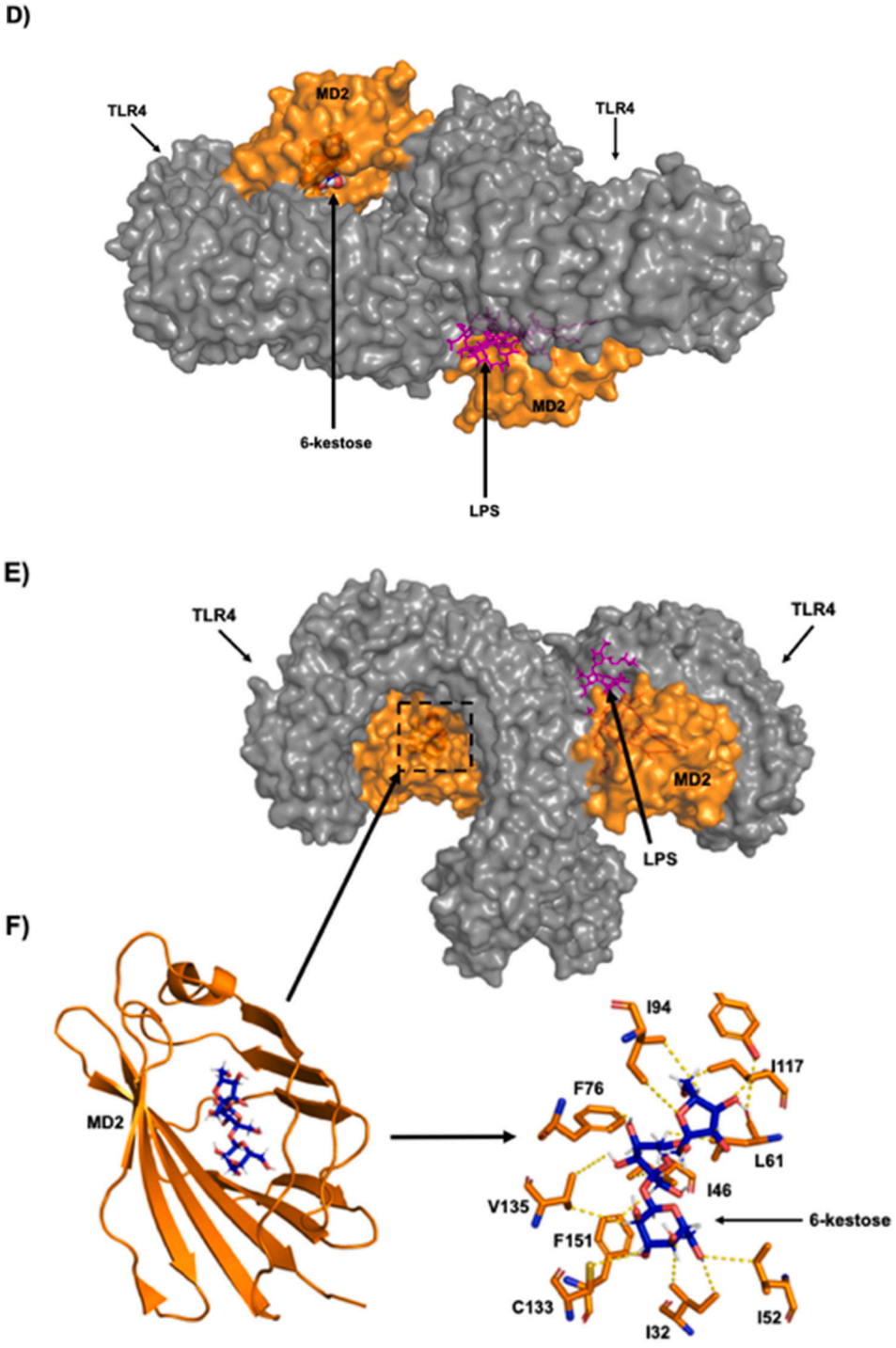

Fig. 8. (*continued*).

described for interaction with the natural agonist of TLR3, such as H39, H60, F84 and H108 (Fig. 9f) (Choe et al., 2005). On the other hand, GF_{10}-inulin, was located at the glycosylated face of TLR3 (Fig. 9g–h). GF_{10}-inulin was found interacting with polar amino acid residues such as E189 and R222, as well as hydrophobic amino acid residues such as I220, L243 and F217 (Fig. 9i). It was different GF_{10}-agavin, which was found at the N-terminal end of TLR3 (Fig. 9j–k), and the key arginine 64 was one of the amino acid residues which established an interaction with GF_{10}-agavin (Fig. 9l).

3.6. Fructans induce branching and structure-dependent inhibitory effects on cytokine production of TLR2 and TLR4 stimulated DCs

Dendritic cells are key players in the gut mucosal immune system and are distributed along the intestinal epithelium (Rescigno et al., 2001). We therefore investigated whether the fructans can also influence cytokine production of DCs. To that end, we incubated DCs for 48 h in the presence and absence of the fructans and determined cytokine release. However, as shown in Fig. S2, the fructans as such did not change cytokine production of DCs (Fig. S2). Since a strong inhibitory effect of the activation of TLR2 and TLR4 was found in HEK-cells, we

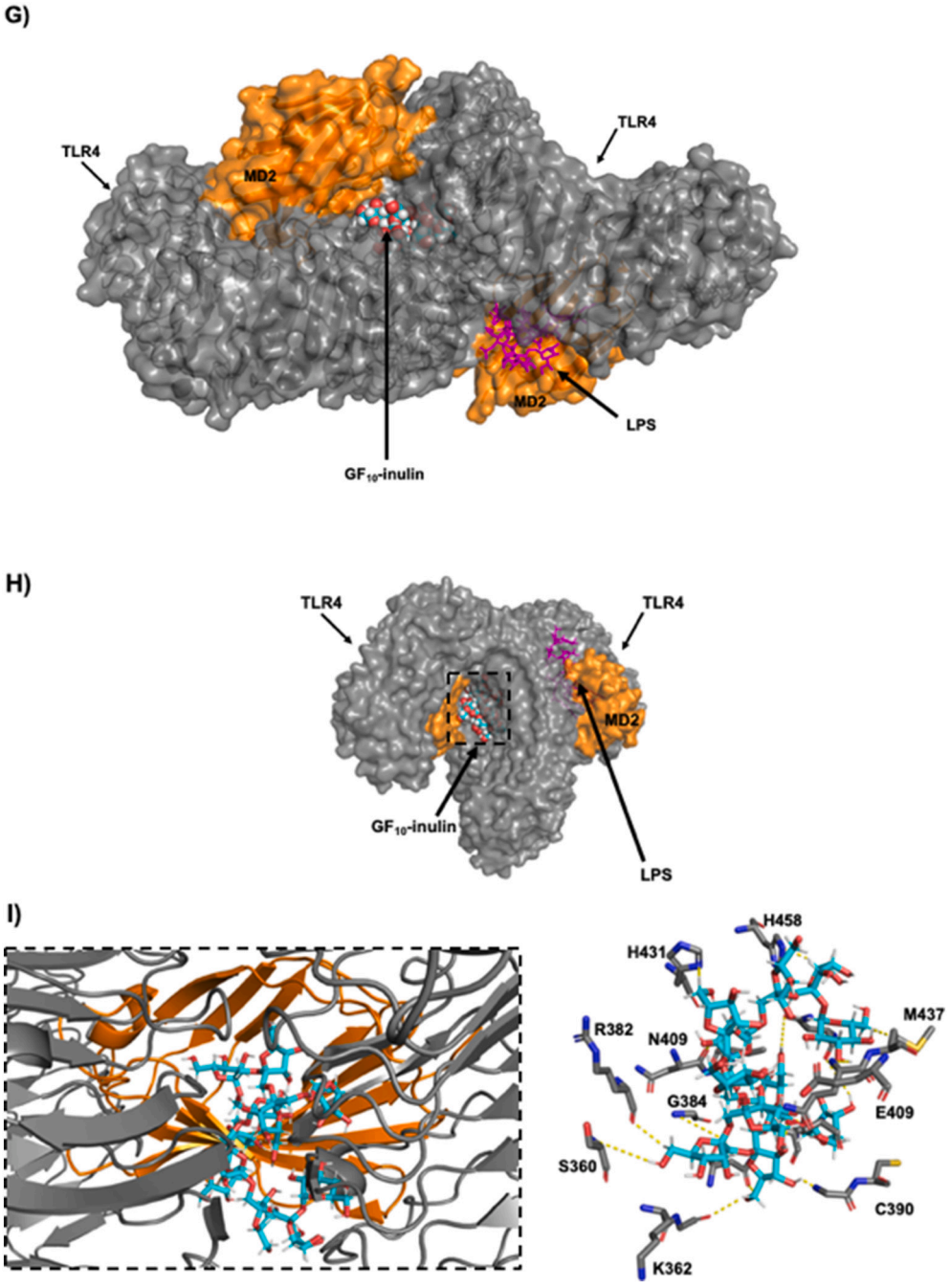

Fig. 8. (*continued*).

investigated in a next set of experiments whether fructans may reduce inflammatory responses induced by agonists for these two TLRs. Therefore, we pre-incubated DCs for 1 h with fructans followed by a stimulation with a combination of TLR2 agonists (FSL-1 and Pam3CSK4) and the TLR4 agonist LPS.

Pre-incubation of DCs with fructans caused attenuation of the inflammatory effect of the TLR2 agonist. ITF I only had a minor effect on the TLR2 induced release of TNFα by DCs (Fig. 10a). This was different for ITF II, which induced a 0.52-fold reduction ($p < 0.05$) in the TLR2 induced TNFα release. The pre-incubation of DCs with GTF I induced a 0.51-fold reduction ($p < 0.05$) in the production of TLR2 induced pro-inflammatory cytokine TNFα release. However, pre-incubation of DCs with GTF II did not induce a significant decrease of TLR2 induced TNFα production (Fig. 10a). No significant differences were found when DCs were preincubated with the fructans for production of MCP-1/CCL2, MIP-1α/CCL3, IL-1RA, IL-1β, IL-6 and IL-10 (Fig. S3a–f).

We also studied the effect of fructans on the cytokine production of DCs when stimulated with the TLR4 agonist LPS. ITF I had no significant effect on chemokine ligand of monocyte chemoattractant protein-1 (MCP-1)/CC (CCL2) (Fig. 10b). However, pre-incubation of ITF II followed by the addition of LPS, caused a decrease of 0.34-fold MCP-1/CC (CCL2) ($p < 0.001$) in TLR4 stimulated DCs. GTF I strongly attenuated MCP-1/CC (CCL2) in the TLR4 stimulated DCs with a 0.41-fold ($p < 0.0001$) reduction. Similar results were found for the pre-incubation of DCs with GTF II, which induced a 0.32-fold decrease ($p < 0.001$) in the TLR4 stimulated DCs (Fig. 10b).

The production of TNFα was not decreased when TLR4 stimulated DCs were pre-incubated with ITF I. This was different for GTF I, since the

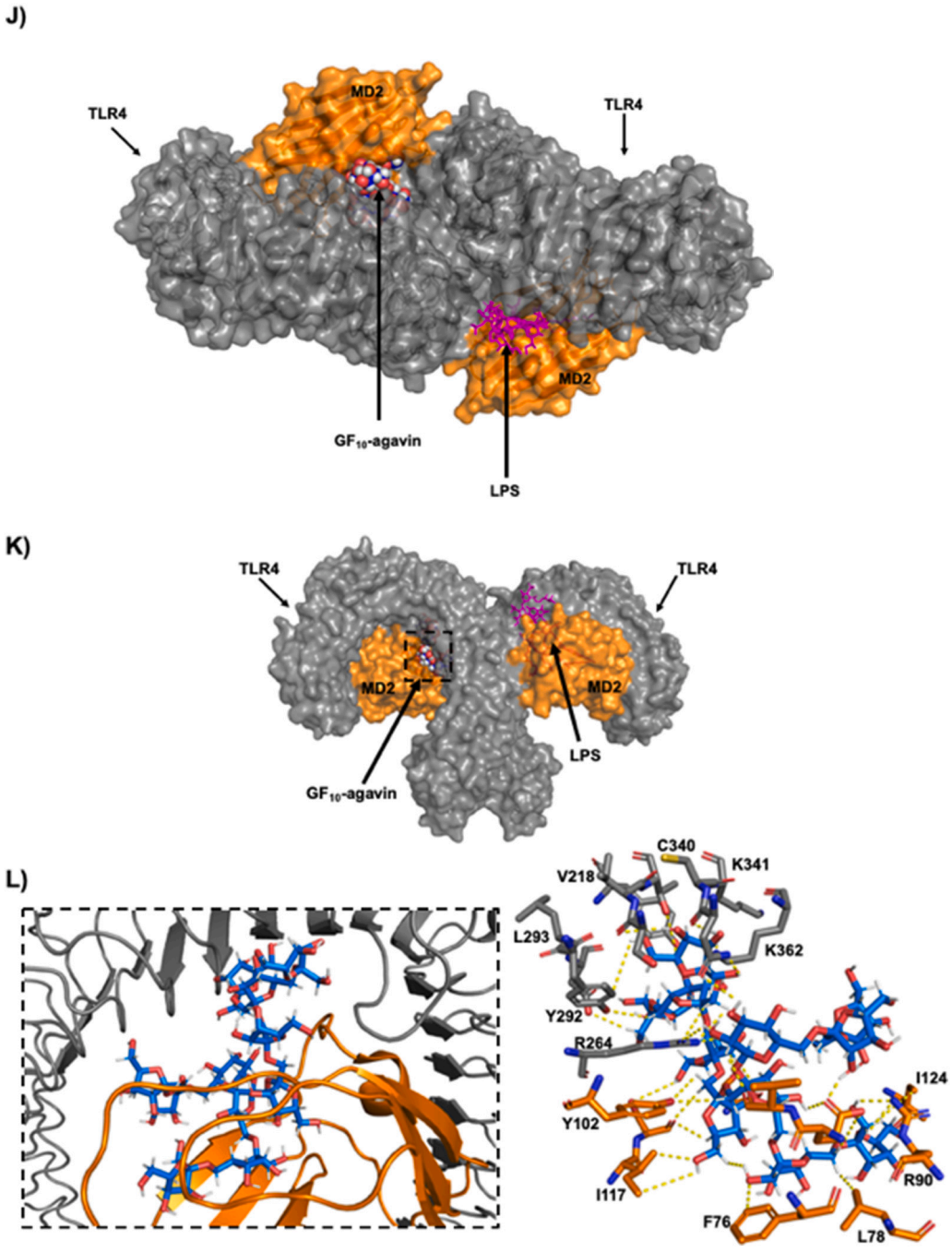

Fig. 8. (*continued*).

production of TNFα was 0.66-fold decreased ($p < 0.05$) in TLR4 stimulated DCs (Fig. 10c). A tendency to decrease the TNFα production was also observed in TLR4 stimulated DCs exposed to ITF II (0.73-fold, $p < 0.1$). This finding was different with GTF II, since no decrease in the production of TNFα was observed in TLR4 stimulated DCs (Fig. 10c). For IL6 we found no statistical lowered production in TLR4-stimulated DCs although GTF I showed a tendency to decrease with a fold change of 0.69 ($p < 0.1$) (Fig. S4d).

4. Discussion

The chemical structure and chain length of branched β(2→1)/β(2→6)-linked fructans from *Agave tequilana* and linear β(2→1)-linked fructans from *Cichorium intybus* were investigated and compared for immunomodulating effects via TLRs. We show that GTFs especially stimulate TLRs 3, 7 and 9 while they were also able to inhibit TLR2 and TLR4. Also, by performing in silico docking studies we identified the ligand binding sites for ITFs and GTFs on TLRs. To the best of our knowledge, this is the first study that demonstrates the direct effect of GTFs on human TLR signaling, their modes of interaction, as well as their influence on cytokine production in TLR2 and TLR4 stimulated dendritic cells.

In this study we investigated both the MyD88 and TRIF dependent pathways that might be influenced by fructans. MyD88 is involved in the signaling of all TLRs except TLR3 and endosomal TLR4 while TRIF signaling is involved in TLR3 and endosomal TLR4 activation (Yamamoto et al., 2003). When testing the stimulation of TLRs by GTFs, we found that in contrast to ITFs the downstream pathway followed for NF-

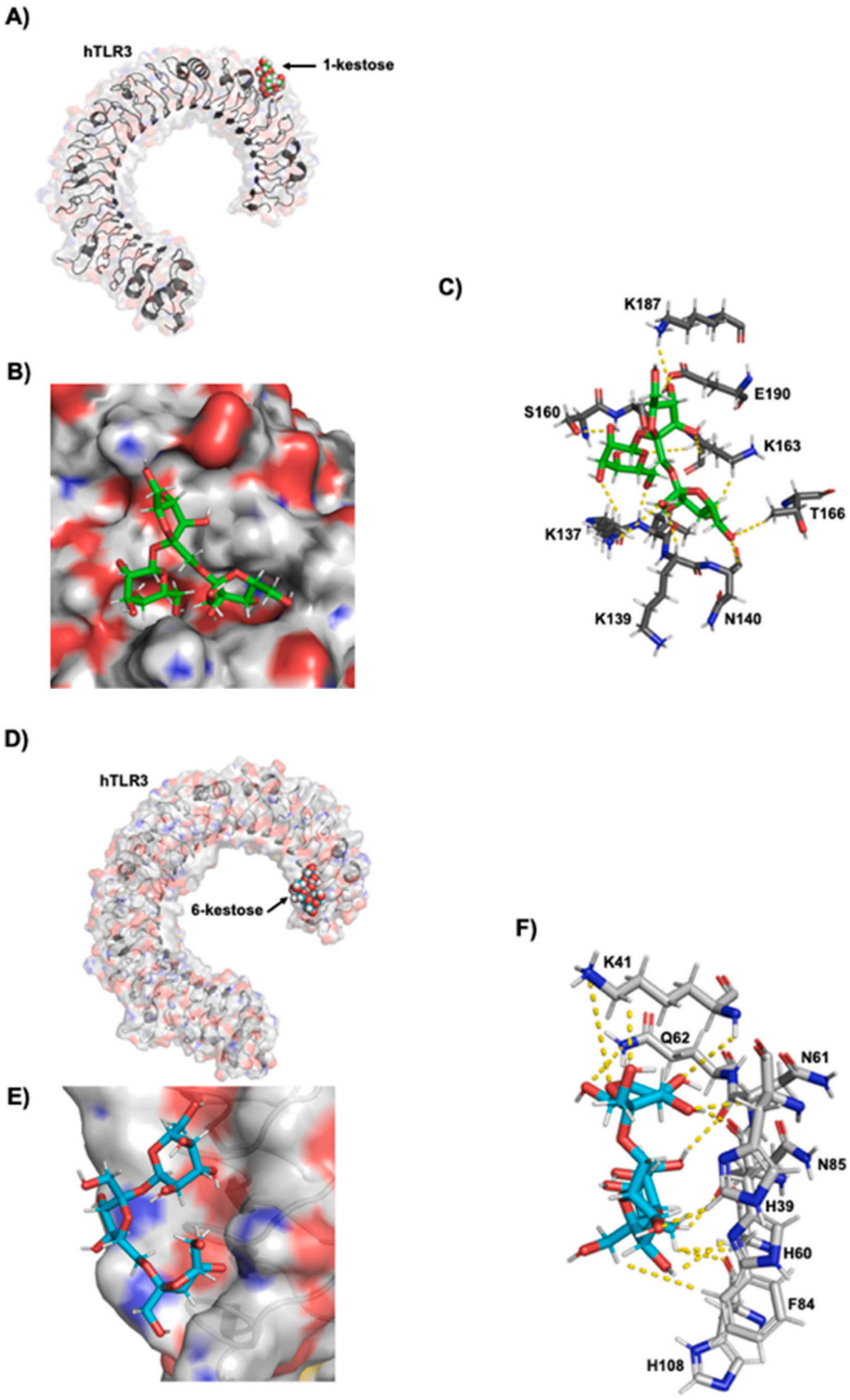

Fig. 9. Molecular interactions predicted between fructans and TLR3. 1-kestose was found to be located at the non-glycosylated side face of TLR3 (A–C). 6-kestose was located at the N-terminal end of TLR3 (D–F). GF_{10}-inulin was found located at the glycosylated face of TLR3 (G–I). GF_{10}-agavin was found at the N-terminal end of TLR3 (J–L).

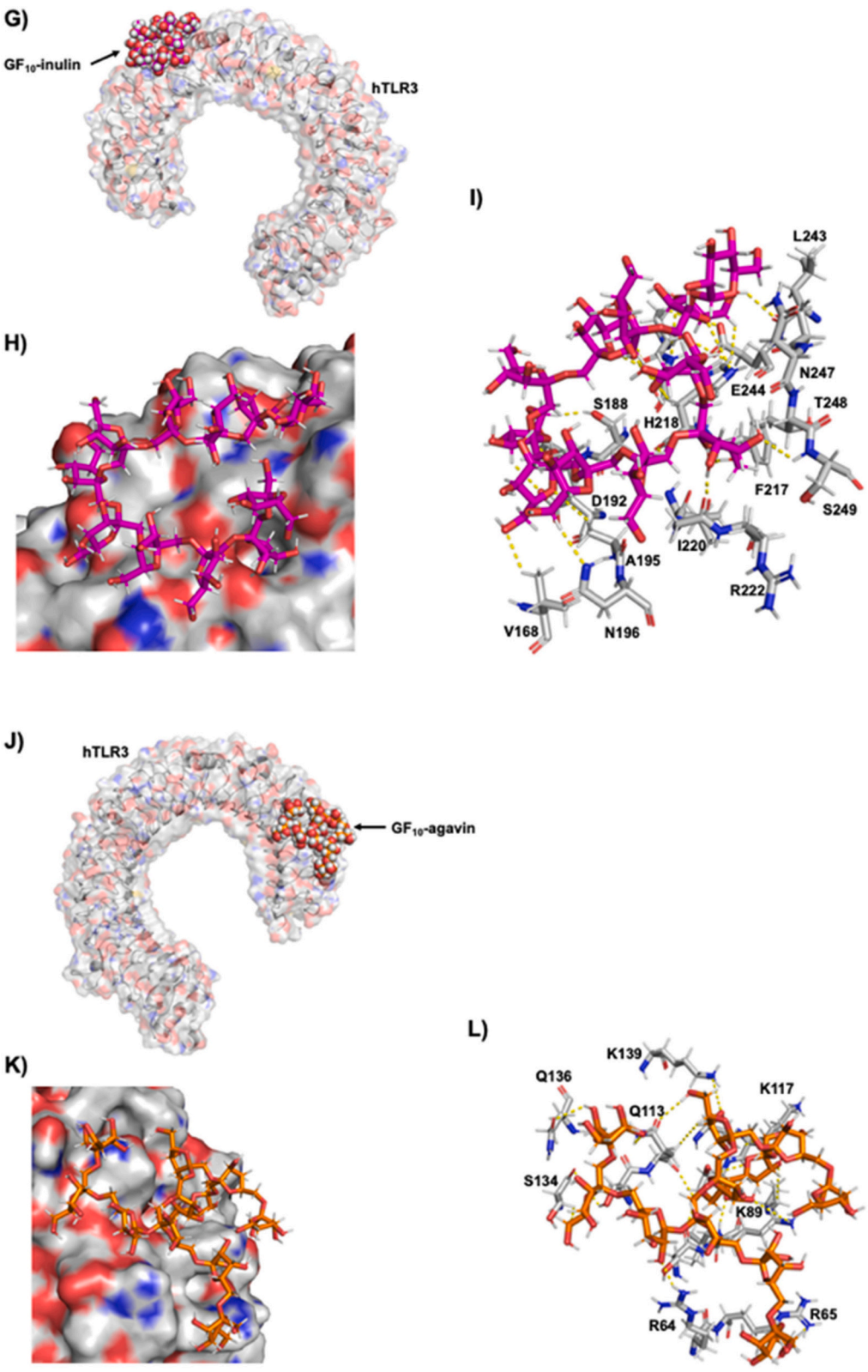

Fig. 9. (*continued*).

κB/AP-1 activation was different between both GTFs. When adding MyD88 inhibitor peptide to GTF I, the activation of NF-κB/AP-1 was completely lost which was different for GTF II where activation of NF-κB/AP-1 was only inhibited when adding the TRIF inhibitor. Thus, we show that GTF II not only depends on MyD88 but also on TRIF pathway for TLR signaling. As the main difference between GTFI and GTFII is the presence of molecules above DP 60 in GTF II, our data suggest that differences observed in the downstream signaling pathways of GTFs is dependent on the differences in structure between them.

Not only different pathways but also different TLRs were activated and inhibited by the fructans in a structure dependent way. The capacity to recognize a broad panel of ligands by TLRs is caused and determined

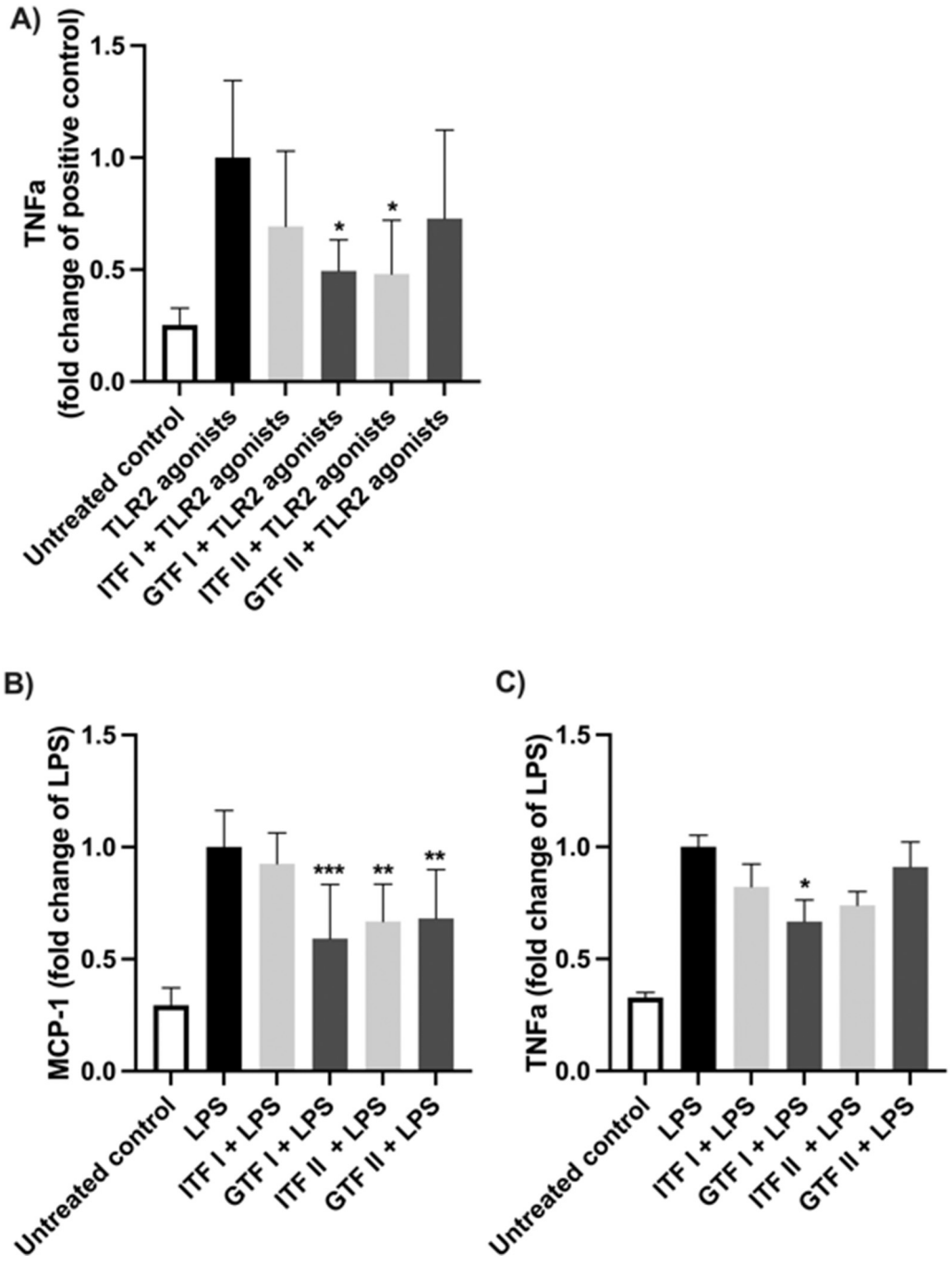

Fig. 10. Cytokine production (fold change of positive control) by dendritic cells pre-treated with GTFs and ITFs and stimulated with TLR2 and TLR4 agonists. * represent statistical differences between positive control and the different treatments (*$p < 0.05$, **$p < 0.01$, ***$p < 0.001$, ****$p < 0.0001$), p-values < 0.1 were considered as a trend.

by the leucine rich repeats (LRR) scaffold in TLRs which can accommodate a broad diversity of structures (Bell et al., 2005). When comparing the capacity of ITFs and GTFs to activate TLRs in HEK-Blue cell lines we found that ITFs and GTFs activate different TLRs. ITFs stimulated TLRs which were dependent on the MyD88 pathway such as TLR2 and 4 which corroborates our previous findings (Vogt et al., 2013) but a different and stronger activation was observed with GTFs that stimulated TRIF dependent TLRs such as TLR3, TLR7 and TLR9. This illustrated again the structure dependent immunomodulating effects of fructans.

Not only activation but also inhibition of TLR signaling was observed by GTFs. In several studies it has been shown that this capacity of food components is functional and can attenuate inflammatory responses (Kiewiet et al., 2018). Especially GTFs had a strong inhibitory effect on activation of TLR2 and TLR4. To gain insight in how GTFs can have such a strong inhibitory effect, we performed molecular docking studies to identify the site of interaction of representative molecules with TLRs. For TLR2, we studied how fructans can interact with binding to its heterodimer with TLR1 which is essential for TLR2 induced immune activation and cytokine release (Jin et al., 2007). This study demonstrates that 6-kestose can bind within the pocket of TLR2 where the natural agonist of its receptor Pam3CSK4 normally binds to the TLR2-1 heterodimer. This finding suggests that 6-kestose prevents binding of TLR2-1 ligands such as Pam3CSK4 to activate TLR2. GF_{10}-agavin was

found outside of the entrance for TLR2 agonist partially blocking this pocket. Moreover, this molecule established contact with Y326 residue, which has been described as a key residue for agonist binding to TLR2 (Jin et al., 2007). These findings suggest that both studied molecules possess the ability to avoid the binding of agonist to TLR2, although the site of binding is structure dependent.

Interaction of 1-kestose and GF_{10}-inulin with TLR2 was also observed but this was not in the ligand binding sites of TLR2-1 but in the heterodimer interface for 1-kestose, and in the central ectodomain for GF_{10}-inulin, which therefore could explain the observed lack of inhibitory effect but mild activating effects, which has been reported before (Vogt et al., 2013). These differences in the inhibition capacity between the studied fructans, might be related to the presence of β(2→6) bonds and the branched structure of GTFs, since GTFs' branched structure is more similar to the branched configuration of the lipid chains that normally fit in the TLR2 pocket (Jin et al., 2007).

GTFs also exerted a strong inhibitory effect on TLR4. Activation of TLR4 requires the formation of a heterodimer with MD2 protein (Park et al., 2009). The natural agonist of TLR4 is LPS (Kim et al., 2007) which binds to TLR4-MD2 complex through its acyl non-polar chains. Parts of these chains exert hydrophobic interactions with the TLR4-MD2 pocket which facilitates the dimerization. Our docking studies demonstrate the unique capacity of 6-kestose and GF_{10}-agavin to interact with key residues for the formation of the TLR4-MD2 complex or for the binding of LPS such as I32, I46 and I94 and I124, by which it can inhibit the TLR4 activation induced by LPS. 1-kestose and GF_{10}-inulin interacted differently with TLR4 and MD2. 1-kestose only interacted with MD2 residues such as L78 and F147, while GF_{10}-inulin only interacted with TLR4 residues such as H458 and G384. Moreover, none of these interactions were with key-amino acids involved in activation of the receptor or formation of the heterodimer. Again, this prediction could illustrate the characteristic properties of β(2→6) fructans to inhibit signaling of some proinflammatory TLRs.

Findings were different with TLR3. Preincubation with GTFs induced a stronger effect of the agonist for TLR3 rather than an inhibition illustrating the synergistic effect of the agonist and GTFs. Our docking studies revealed that 6-kestose and GF_{10}-agavin interacted with residues of TLR3 which have been previously described as key residues for interaction of this receptor with its natural agonist (Bell et al., 2005; Choe et al., 2005). The natural agonist of TLR3 is viral double stranded RNA (Bell et al., 2005; Choe et al., 2005). It has also been proposed that phosphate and ribose sugar moieties of RNA are responsible for interactions and activation of TLR3 (Bell et al., 2005). The structural similarities between ribose arrangement in RNA helix and the fructose units in GTFs with β(2→6) bonds and branched structure might explain the recognition of these polysaccharides by TLR3 and its over stimulation. This was different with 1-kestose and GF_{10}-inulin, since these molecules established interactions with amino acid residues located at the glycosylated face and the N-terminal end of TLR3. These glycosylated sites represent a steric hindrance for the binding of the agonist to TLR3 (Bell et al., 2005). Thus, this might be the explanation for the absence of interaction between ITFs and TLR3.

Dendritic cells are key players in the intestine immunity and are able to distinguish harmful from harmless antigens (Mowat, 2003; Rescigno et al., 2001; Sato & Iwasaki, 2005). They are equipped with TLRs and overactivation may lead to several intestinal and systemic disorders (Mowat, 2003). We therefore next tested whether ITFs are able to manage inflammatory responses by attenuating TLR2-1 and TLR4 induced responses in dendritic cells. As such the fructans did not change cytokines of unstimulated dendritic cells which corroborates previous findings (Bermudez-Brito et al., 2015). This was different in TLR2 and TLR4 stimulated dendritic cells. Both types of GTFs as well as ITFII had a profound inhibitory effect on TLR2 and TLR4 induced immune activation of dendritic cells. GTF I also exerted a reduction in the production of the chemokine ligand of monocyte chemoattractant protein-1 (MCP-1)/CC (CCL2) induced by TLR induced activation. This attenuation aligns with the findings of the docking studies and could possibly also be an explanation for the modulation in release of proinflammatory cytokines by immune cells described for other polysaccharides with prebiotic activity, such as galacto-oligo-saccharides, goat milk oligosaccharides and also fructooligosaccharides and inulins (Capitán-Cañadas et al., 2014).

In summary our findings may explain the mechanisms by which immunomodulating food ingredients such as agave fructans with β(2→6) bonds beneficially modulate immune responses (Bermudez-Brito et al., 2015; Vogt et al., 2013; Vogt et al., 2014). Agave plants are endemic in the Latin American region (López-Romero et al., 2018) and often used as an affordable source for obtaining fructans for food supplementation to support health. However, our data also suggest that the structure of fructans should be carefully determined and taken into consideration when intended to be used as food supplement as we show that the presence of linear or branched structure, the chain-length, as well as the dose of these molecules can exert differential responses. Further studies are needed in order to establish specifically in which disease state agave fructans could serve as an alternative or supplemental therapeutic option (Liu et al., 2004). As TLR2 and TLR4 signaling have been shown to be involved in mucositis and other intestinal disorders our data suggest that GTFs and ITF II have beneficial effects on these disorders. This suggestion is supported by a recent observation that ITF II supported gastrointestinal health in aged individuals (Kiewiet et al., 2021). Overall our study shows that beneficial immunomodulatory effects of GTFs may be explained by its impact on TLRs and attenuation of proinflammatory responses.

CRediT authorship contribution statement

C. Fernández-Lainez: Conceptualization, Methodology, Investigation, Formal analysis, Software, Writing – original draft. **R. Akkerman:** Methodology, Writing – review & editing. **M.M.P. Oerlemans:** Methodology, Writing – review & editing. **M.J. Logtenberg:** Methodology, Writing – review & editing. **H.A. Schols:** Conceptualization, Methodology, Formal analysis, Writing – review & editing. **L.A. Silva-Lagos:** Methodology, Writing – review & editing. **G. López-Velázquez:** Conceptualization, Methodology, Formal analysis, Software, Writing – review & editing. **P. de Vos:** Conceptualization, Writing – review & editing, Supervision, Project administration.

Declaration of competing interest

The authors declare no conflict of interest.

Acknowledgements

This study was partially financed by the "Programa de Recursos Fiscales para Investigación" from Instituto Nacional de Pediatría, Grant number 2019/062. C.F.L. was financially supported by Abel Tasman Talent Program Sandwich PhD from the University of Groningen-University Medical Center Groningen, UG/UMCG in collaboration with Universidad Nacional Autónoma de México, UNAM and CONACyT (#260625).

Appendix A. Supplementary data

Supplementary data to this article can be found online at https://doi.org/10.1016/j.carbpol.2021.118893.

References

Abreu, M. T. (2010). Toll-like receptor signalling in the intestinal epithelium: How bacterial recognition shapes intestinal function. *Nature Reviews Immunology, 10*, 131–144.

Beaglehole, R., Bonita, R., Horton, R., Adams, C., Alleyne, G., Asaria, P., & Casswell, S. (2011). Priority actions for the non-communicable disease crisis. *The Lancet, 377* (9775), 1438–1447.

Bell, J. K., Botos, I., Hall, P. R., Askins, J., Shiloach, J., Segal, D. M., & Davies, D. R. (2005). The molecular structure of the toll-like receptor 3 ligand-binding domain. *Proceedings of the National Academy of Sciences, 102*(31), 10976–10980.

Berman, H. M., Westbrook, J., Feng, Z., Gilliland, G., Bhat, T. N., Weissig, H., & Bourne, P. E. (2000). The protein data bank. *Nucleic Acids Research, 28*(1), 235–242.

Bermudez-Brito, M., Sahasrabudhe, N. M., Rösch, C., Schols, H. A., Faas, M. M., & de Vos, P. (2015). The impact of dietary fibers on dendritic cell responses in vitro is dependent on the differential effects of the fibers on intestinal epithelial cells. *Molecular Nutrition & Food Research, 59*(4), 698–710.

Capitán-Cañadas, F., Ortega-González, M., Guadix, E., Zarzuelo, A., Suárez, M. D., de Medina, F. S., & Martínez-Augustin, O. (2014). Prebiotic oligosaccharides directly modulate proinflammatory cytokine production in monocytes via activation of TLR 4. *Molecular Nutrition & Food Research, 58*(5), 1098–1110.

Cheng, L., Kiewiet, M. B., Groeneveld, A., Nauta, A., & de Vos, P. (2019). Human milk oligosaccharides and its acid hydrolysate LNT2 show immunomodulatory effects via TLRs in a dose and structure-dependent way. *Journal of Functional Foods, 59*, 174–184.

Choe, J., Kelker, M. S., & Wilson, I. A. (2005). Crystal structure of human toll-like receptor 3 (TLR3) ectodomain. *Science, 309*(5734), 581–585.

DeLano, W. L. (2002). Pymol: An open-source molecular graphics tool. *CCP4 Newsletter on Protein Crystallography, 40*(1), 82–92.

Filippov, I. V., & Nicklaus, M. C. (2009). Optical structure recognition software to recover chemical information: OSRA, an open source solution. *Journal of Chemical Information and Modeling, 49*(3), 740–743.

Flamm, G., Glinsmann, W., Kritchevsky, D., Prosky, L., & Roberfroid, M. (2001). Inulin and oligofructose as dietary fiber: A review of the evidence. *Critical Reviews in Food Science and Nutrition, 41*(5), 353–362.

Gay, N. J., & Gangloff, M. (2007). Structure and function of toll receptors and their ligands. *Annual Review of Biochemistry, 76*, 141–165.

Grosdidier, A., Zoete, V., & Michielin, O. (2011). SwissDock, a protein-small molecule docking web service based on EADock DSS. *Nucleic Acids Research, 39*(suppl_2), W270–W277.

Hanwell, M. D., Curtis, D. E., Lonie, D. C., Vandermeersch, T., Zurek, E., & Hutchison, G. R. (2012). Avogadro: An advanced semantic chemical editor, visualization, and analysis platform. *Journal of Cheminformatics, 4*(1), 1–17.

Health, U. D.o., & Services, H. (2015). *US Department of Agriculture. 2015–2020 dietary guidelines for Americans. Washington, DC*.

Jin, M. S., Kim, S. E., Heo, J. Y., Lee, M. E., Kim, H. M., Paik, S.-G., & Lee, J.-O. (2007). Crystal structure of the TLR1-TLR2 heterodimer induced by binding of a tri-acylated lipopeptide. *Cell, 130*(6), 1071–1082.

Kiewiet, M. B., Rodríguez, M. I. G., Dekkers, R., Gros, M., Ulfman, L. H., Groeneveld, A., & Faas, M. M. (2018). The epithelial barrier-protecting properties of a soy hydrolysate. *Food & Function, 9*(8), 4164–4172.

Kiewiet, M. B. G., Elderman, M. E., El Aidy, S., Burgerhof, J. G. M., Visser, H., Vaughan, E. E., & de Vos, P. (2021). Flexibility of gut microbiota in ageing individuals during dietary fiber long-chain inulin intake. *Molecular Nutrition & Food Research, 65*(4), 2000390.

Kim, H. M., Park, B. S., Kim, J.-I., Kim, S. E., Lee, J., Oh, S. C., & Yoo, O. J. (2007). Crystal structure of the TLR4-MD-2 complex with bound endotoxin antagonist eritoran. *Cell, 130*(5), 906–917.

Kim, S., Chen, J., Cheng, T., Gindulyte, A., He, J., He, S., & Yu, B. (2019). PubChem 2019 update: Improved access to chemical data. *Nucleic Acids Research, 47*(D1), D1102–D1109.

Krieger, E., Joo, K., Lee, J., Lee, J., Raman, S., Thompson, J., & Karplus, K. (2009). Improving physical realism, stereochemistry, and side-chain accuracy in homology modeling: Four approaches that performed well in CASP8. *Proteins: Structure, Function, and Bioinformatics, 77*(S9), 114–122.

Lépine, A., & de Vos, P. (2018). Synbiotic effects of the dietary fiber long-chain inulin and probiotic lactobacillus acidophilus W37 can be caused by direct, synergistic stimulation of immune toll-like receptors and dendritic cells. *Molecular Nutrition & Food Research, 62*(15), 1800251.

Liu, F., Liu, Y., Meng, Y., Yang, M., & He, K. (2004). Structure of polysaccharide from polygonatum cyrtonema hua and the antiherpetic activity of its hydrolyzed fragments. *Antiviral Research, 63*(3), 183–189.

López, M. G., & Urías-Silvas, J. E. (2007). Agave fructans as prebiotics. *Recent Advances in Fructooligosaccharides Research, 37*, 1–14.

Lopez, M. G., Mancilla-Margalli, N. A., & Mendoza-Diaz, G. (2003). Molecular structures of fructans from Agave tequilana Weber var. Azul. *Journal of Agricultural and Food Chemistry, 51*(27), 7835–7840.

López-Romero, J. C., Ayala-Zavala, J. F., González-Aguilar, G. A., Peña-Ramos, E. A., & González-Ríos, H. (2018). Biological activities of agave by-products and their possible applications in food and pharmaceuticals. *Journal of the Science of Food and Agriculture, 98*(7), 2461–2474.

López-Velázquez, G., Parra-Ortiz, M., de la Mora-de la Mora, I., García-Torres, I., Enríquez-Flores, S., Alcántara-Ortigoza, M. A., & Cruz-Rubio, J. M. (2015). Effects of fructans from Mexican agave in newborns fed with infant formula: a randomized controlled trial. *Nutrients, 7*(11), 8939–8951.

Mancilla-Margalli, N. A., & López, M. G. (2006). Water-soluble carbohydrates and fructan structure patterns from agave and dasylirion species. *Journal of Agricultural and Food Chemistry, 54*(20), 7832–7839.

Mowat, A. M. (2003). Anatomical basis of tolerance and immunity to intestinal antigens. *Nature Reviews Immunology, 3*(4), 331–341.

Oerlemans, M. M., Akkerman, R., Ferrari, M., Walvoort, M. T., & de Vos, P. (2020). Benefits of bacteria-derived exopolysaccharides on gastrointestinal microbiota, immunity and health. *Journal of Functional Foods, 104289*.

Park, B. S., Song, D. H., Kim, H. M., Choi, B.-S., Lee, H., & Lee, J.-O. (2009). The structural basis of lipopolysaccharide recognition by the TLR4–MD-2 complex. *Nature, 458*(7242), 1191–1195.

Patry, R. T., & Nagler, C. R. (2021). Fiber-poor Western diets fuel inflammation. *Nature Immunology*, 1–3.

Pérez-López, A. V., & Simpson, J. (2020). The sweet taste of adapting to the desert: Fructan metabolism in agave species. *Frontiers in Plant Science, 11*, 324.

Pettersen, E. F., Goddard, T. D., Huang, C. C., Couch, G. S., Greenblatt, D. M., Meng, E. C., & Ferrin, T. E. (2004). UCSF Chimera—a visualization system for exploratory research and analysis. *Journal of Computational Chemistry, 25*(13), 1605–1612.

Rescigno, M., Urbano, M., Valzasina, B., Francolini, M., Rotta, G., Bonasio, R., & Ricciardi-Castagnoli, P. (2001). Dendritic cells express tight junction proteins and penetrate gut epithelial monolayers to sample bacteria. *Nature Immunology, 2*(4), 361–367.

Roberfroid, M. B. (2005). Introducing inulin-type fructans. *British Journal of Nutrition, 93*(S1), S13–S25.

Roberfroid, M. B., Van Loo, J. A., & Gibson, G. R. (1998). The bifidogenic nature of chicory inulin and its hydrolysis products. *The Journal of Nutrition, 128*(1), 11–19.

Sahasrabudhe, N. M., Beukema, M., Tian, L., Troost, B., Scholte, J., Bruininx, E., & Schols, H. A. (2018). Dietary fiber pectin directly blocks toll-like receptor 2–1 and prevents doxorubicin-induced ileitis. *Frontiers in Immunology, 9*, 383.

Sato, A., & Iwasaki, A. (2005). Peyer's patch dendritic cells as regulators of mucosal adaptive immunity. *Cellular and Molecular Life Sciences, 62*(12), 1333–1338.

Takeda, K., & Akira, S. (2004). TLR signaling pathways. *Seminars in Immunology, 16*, 3–9. Elsevier.

Temba, G. S., Kullaya, V., Pecht, T., Mmbaga, B. T., Aschenbrenner, A. C., Ulas, T., & Kumar, V. (2021). Urban living in healthy tanzanians is associated with an inflammatory status driven by dietary and metabolic changes. *Nature Immunology, 22*(3), 287–300.

Van den Abbeele, P., Duysburgh, C., Ghyselinck, J., Goltz, S., Berezhnaya, Y., Boileau, T., & Marzorati, M. (2021). Fructans with varying degree of polymerization enhance the selective growth of bifidobacterium animalis subsp. Lactis BB-12 in the human gut microbiome in vitro. *Applied Sciences, 11*(2), 598.

Van den Ende, W. (2013). Multifunctional fructans and raffinose family oligosaccharides. *Frontiers in Plant Science, 4*, 247.

Veronese, N., Solmi, M., Caruso, M. G., Giannelli, G., Osella, A. R., Evangelou, E., & Tzoulaki, I. (2018). Dietary fiber and health outcomes: An umbrella review of systematic reviews and meta-analyses. *The American Journal of Clinical Nutrition, 107*(3), 436–444.

Versluys, M., Kirtel, O., Toksoy Öner, E., & Van den Ende, W. (2018). The fructan syndrome: Evolutionary aspects and common themes among plants and microbes. *Plant, Cell & Environment, 41*(1), 16–38.

Vijn, I., & Smeekens, S. (1999). Fructan: More than a reserve carbohydrate? *Plant Physiology, 120*(2), 351–360.

Vogt, L., Ramasamy, U., Meyer, D., Pullens, G., Venema, K., Faas, M. M., & de Vos, P. (2013). Immune modulation by different types of β2→ 1-fructans is toll-like receptor dependent. *PLoS One, 8*(7), Article e68367.

Vogt, L. M., Meyer, D., Pullens, G., Faas, M. M., Venema, K., Ramasamy, U., & de Vos, P. (2014). *Toll-Like Receptor 2 Activation by b2→ 1-Fructans Protects Barrier Function of T84 Human Intestinal Epithelial Cells in a Chain Length–Dependent Manner*.

Vogt, L. M., Elderman, M. E., Borghuis, T., de Haan, B. J., Faas, M. M., & de Vos, P. (2017). Chain length-dependent effects of inulin-type fructan dietary fiber on human systemic immune responses against hepatitis-B. *Molecular Nutrition & Food Research, 61*(10), 1700171.

Yamamoto, M., Sato, S., Hemmi, H., Hoshino, K., Kaisho, T., Sanjo, H., & Takeda, K. (2003). Role of adaptor TRIF in the MyD88-independent toll-like receptor signaling pathway. *Science, 301*(5633), 640–643.